METEOR-Berichte

Surface Ocean – Lower Atmosphere Study (SOLAS) in the upwelling region off Peru

Cruise No. M91

December 01 – December 26, 2012
Callao (Peru) – Callao (Peru)

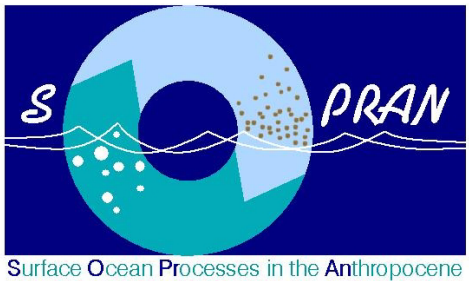

H. W. Bange

Editorial Assistance:

DFG-Senatskommission für Ozeanographie
MARUM – Zentrum für Marine Umweltwissenschaften der Universität Bremen

2013

The METEOR-Berichte are published at irregular intervals. They are working papers for people who are occupied with the respective expedition and are intended as reports for the funding institutions. The opinions expressed in the METEOR-Berichte are only those of the authors.

The METEOR expeditions are funded by the *Deutsche Forschungsgemeinschaft (DFG)* and the *Bundesministerium für Bildung und Forschung (BMBF)*.

Editor:
DFG-Senatskommission für Ozeanographie
c/o MARUM – Zentrum für Marine Umweltwissenschaften
Universität Bremen
Leobener Strasse
28359 Bremen

Author:
PD Dr. Hermann Bange
Chemische Ozeanographie
GEOMAR
Düsternbrooker Weg 20
24105 Kiel, Germany

Telefon: +49 431 600 4204
Telefax: +49 431 600 4202
e-mail: hbange@geomar.de

Citation: H.W. Bange (2013) Surface Ocean – Lower Atmosphere Study (SOLAS) in the upwelling region off Peru - Cruise No. M91 – December 01 – December 26, 2012 – Callao (Peru) – Callao (Peru). METEOR-Berichte, M91, 69 pp., DFG-Senatskommission für Ozeanographie, DOI:10.2312/cr_m91

ISSN 2195-8475

Table of Contents

1 Summary

The Meteor cruise M91 (Callao-Callao) took place off Peru from 01 December to 26 December 2012. The overall goal of M91 was to conduct an integrated biogeochemical study on the upwelling region off Peru in order to assess its importance for the emissions of various climate-relevant atmospheric trace gases and tropospheric chemistry. The various work packages of M91 included measurements of and sampling for (1) atmospheric and dissolved trace gases, (2) aerosols, (3) nitrogen processes and isotopes in the water column, (4) dissolved organic matter in the surface microlayer, (5) upwelling velocity, and (6) exchange fluxes across the ocean/atmosphere interface. M91 was funded by the German BMBF 'Verbundprojekt' SOPRAN (Surface Ocean Processes in the Anthropocene) which is a German contribution to SOLAS (Surface Ocean – Lower Atmosphere Study).

Zusammenfassung

Die Meteorfahrt M91 (Callao-Callao) fand vom 1. bis 26. Dezember 2012 vor Peru statt. Das übergeordnete Ziel von M91 war, eine umfassende biogeochemische Studie des Auftriebsgebiets vor Peru durchzuführen, um die Bedeutung dieses Gebietes für die Emissionen von klimarelevanten Spurengasen und die Chemie der Troposphäre abzuschätzen. Die verschiedenen Arbeitspakete von M91 umfassten sowohl Messungen als auch Beprobung von 1. Spurengasen in der Wassersäule und in der Atmosphäre, 2. Aerosolen, 3. Stickstoffprozessen und –isotopen in der Wassersäule, 4. gelöster organische Materie in der (Ozean-)Oberflächengrenzschicht, 5. Auftriebsgeschwindigkeit und 6. Austauschflüssen über die Ozean/Atmosphären-Grenzschicht. M91 wurde finanziert durch das BMBF Verbundprojekt SOPRAN (Surface Ocean Processes in the Anthropocene), dem deutsche Beitrag zu SOLAS (Surface Ocean – Lower Atmosphere Study).

2 Participants

Name	Discipline	Institution	e-mail
PD Dr. Bange, Hermann	Chem. Oceanogr./*Ch.Sci.*	GEOMAR	hbange@geomar.de
Bernales, Avy	Biol. Oceanogr./*Obs.*	IMARPE	abernales@imarpe.gob.pe
Flores, Georgina	Chem. Oceanogr./*Obs.*	IMARPE	gflores@imarpe.gob.pe
Leon, Violeta	Chem. Oceanogr./*Obs.*	IMARPE	vleon@imarpe.gob.pe
Arevalo, Damian	Chem. Oceanography	GEOMAR	darevalo@geomar.de
Baustian, Tina	Chem. Oceanography	GEOMAR	tbaustian@geomar.de
Craig, Joel	Chem. Oceanography	GEOMAR	jcraig@geomar.de
Dr. Fischer, Tim	Phys. Oceanography	GEOMAR	tfischer@geomar.de
Flöter, Sebastian	Chem. Oceanography	GEOMAR	sfloeter@geomar.de
Fuhlbrügge, Steffen	Meteorology	GEOMAR	sfuhlbrügge@geomar.de
Galgani, Luisa	Biol. Oceanography	GEOMAR	lgalgani@geomar.de
Hepach, Helmke	Chem. Oceanography	GEOMAR	hhepach@geomar.de
Ihnenfeld, Verena	Chem. Oceanography	GEOMAR	vihnenfeld@geomar.de
Dr. Kock, Annette	Chem. Oceanography	GEOMAR	akock@geomar.de
Krüger, Matthias	Phys. Oceanography	GEOMAR	mkrueger@geomar.de
Nachtigall, Kerstin	Biol. Oceanography	GEOMAR	knachtigall@geomar.de
Dr. Raimund, Stefan	Chem. Oceanography	GEOMAR	sraimund@geomar.de
Roa, Jon	Biol. Oceanography	GEOMAR	jroa@geomar.de
Rother, Kristian	Phys. Oceanography	GEOMAR	krother@oktopus-mari-tech.de
Derstroff, Bettina	Atmos. Chemistry	MPI CH	bettina.derstroff@mpic.de
Dr. Song, Wei	Chem. Oceanography	MPI CH	wei.song@mpic.de
Dr. Veres, Patrick	Atmos. Chemistry	MPI CH	patrick.veres@mpic.de
Peters, Maike	Phys. Oceanography	U Bremen	maikepeters@hotmail.de
Weinberg, Ingo	Chem. Oceanogrpahy	U Hamburg	ingo.weinberg@zmaw.de
Kiefhaber, Daniel	Atmos. Physics	U Heidelb.	daniel.kiefhaber@iup.uni-heidelberg.de
Lampel, Johannes	Atmos. Physics	U Heidelb.	johannes.lampel@iup.uni-heidelberg.de
Nagel, Leila	Atmos. Physics	U Heidelb.	leila.nagel@iup.uni-heidelberg.de
Martogli, Natascha	Mar. Microbiology	U Kiel	nmartogli@geomar.de
Dr. Bourbonnais, Annie	Mar. Microbiology	U Mass	anniebourbonnais@yahoo.ca
Frey, Bernd	Meteorology	DWD	

Ch.Sci., Chief Scientist; Obs., Observer

List of participating PIs

PI	Affiliation	Topic	e-mail
Prof. Mark Altabet	U Mass	N Isotopes	maltabet@umassd.edu
Prof. Elliot Atlas	RSMAS	atm. Trace gases	eatlas@rsmas.miami.edu
Dr. Alex Baker	UEA	Aerosols	alex.baker@uea.ac.uk
PD Dr. H. Bange	GEOMAR	N_2O	hbange@geomar.de
Prof. Harald Biester	TUB	inorg./partic. Halogens	h.biester@tu-bs.de
Prof. Astrid Bracher	AWI	Pigments	astrid.bracher@awi.de
Dr. Marcus Dengler	GEOMAR	Microstructure	mdengler@geomar.de
Prof. Anja Engel	GEOMAR	Surface microlayer	aengel@geomar.de
Dirk Fleischer	GEOMAR	Data management	dfleischer@geomar.de
Dr. Martin Gade	U Hamburg	SAR pictures	martin.gade@zmaw.de
Dr. Michelle Graco	IMARPE	Carbonate system	mgraco@imarpe.gob.pe
Prof. Bernd Jähne	U Heidelberg	Air/sea exchange	bernd.jaehne@iup.uni-heidelberg.de
Prof. Klaus Jürgens	IOW	Microbiology	klaus.juergens@io-warnemuende.de
PD Dr. K. Krüger	GEOMAR	Meteorology	kkrueger@geomar.de
Dr. Carolin Löscher	U Kiel	N Processes	cloescher@ifam.uni-kiel.de
Prof. Ulrich Platt	U Heidelberg	reactive atm. halogens	ulrich.platt@iup.uni-heidelberg.de
Dr. Falk Pollehne	IOW	Halocarbon isotopes	falk.pollehne@io-warnemuende.de
Dr. Birgit Quack	GEOMAR	diss. halocarbons	bquack@geomar.de
Dr. Richard Seifert	U Hamburg	Halocarbon isotopes	richard.seifert@zmaw.de
Prof. D. Schulz-Bull	IOW	Halocarbon isotopes	detlef.schulz-bull@io-warnemuende.de
Dr. Reiner Steinfeldt	U Bremen	Upwelling velocity	rsteinf@physik.uni-bremen.de
Dr. Tobias Steinhoff	GEOMAR	pCO_2	tsteinhoff@geomar.de
Prof. J. Williams	MPI CH	atm. OVOC, diss. VOC	jonathan.williams@mpic.de
Prof. Ch. Zappa	LDEO	CO_2 Fluxes	zappa@ldeo.columbia.edu
Dr. C. Zindler	GEOMAR	diss. DMS	czindler@geomar.de

DWD	Deutscher Wetterdienst, Hamburg, Germany
GEOMAR	GEOMAR Helmholtz-Zentrum für Ozeanforschung Kiel, Germany
IOW	Leibniz-Institut für Ostseeforschung Warnemünde, Warnemünde, Germany
IMARPE	Instituto del Mar del Peru, Callao, Peru
LDEO	Lamont-Doherty Earth Observatory, Palisades, NY, USA
MPI CH	Max-Planck-Institut für Chemie, Mainz, Germany
RSMAS	The Rosenstiel School of Marine and Atmos. Science, U Miami, Miami, FL, USA
TUB	TU Braunschweig, Germany
U Bremen	Universität Bremen, Germany
UEA	School of Environmental Sciences, Univ. East Anglia, Norwich, UK
U Hamburg	Universität Hamburg, Germany
U Heidelberg	Universität Heidelberg, Germany
U Kiel	Universität Kiel, Germany
U Mass	University of Massachusetts, Dartmouth, MA, USA

3 Research Program

3.1 The overall goal of M91 was

to conduct an integrated biogeochemical study on the upwelling region off Peru in order to assess its importance for the emissions of various climate-relevant atmospheric trace gases and tropospheric chemistry.

Therefore, M91 was designed as a measurement campaign that not only focussed on the ocean/atmosphere exchange, but also on the ocean biogeochemistry of the upper ocean, atmospheric gas and aerosol fluxes as well as atmospheric and oceanographic processes.

3.2 Quick overview of the measurement program

WP Nitrous oxide / short-lived N compounds / N processes
(PIs Hermann Bange, Carolin Löscher)

- Underway dissolved N_2O, CO and CO_2
- Depth profiles of diss. CH_4
- Depth profiles of N_2O, hydroxylamine (NH_2OH), hydrazine (N_2H_4)
- Depth profiles of DNA/RNA, flow cytometry
- N_2O and NH_2OH production rates
- N_2 fixation rates

WP Carbonate system
(PI Michelle Graco)

- pH, DIC, total alkalinity chlorophyll
- Ca, Si isotopes
- Utermöhl samples
- Chlorophyll
- Phytoplankton amount
- Coccolithophorid diversity

WP Microstructure
(PI Marcus Dengler)

- Microstructure profiling system
- Conductivity-temperature-depth (CTD) profiles (incl. fluorescence sensor)
- ADCP measurements

WP Upwelling velocity
(PI Reiner Steinfeldt)

- Helium isotope ratio ($^3He/^4He$)

WP Halocarbons, Radio soundings, Pigments
(PIs Birgit Quack, Kirsten Krüger, Harald Biester, Elliot Atlas)

- Underway and depth profiles of diss. halocarbons

- Atmospheric halocarbons and other trace gases (canister sampling)
- Underway and depth profiles of diss. oxygenated/reduced inorganic and particulate organic halogens
- Phytoplankton pigments
- Flow cytometry
- DNA
- Rain rate, rain drop size, rain amount
- Radio soundings (humidity, air temp., wind speed)

WP Halocarbon isotopes and molecular biology
(PIs Richard Seifert, Detlef Schulz-Bull, Klaus Jürgens, Falk Pollehne)

- Carbon isotopic composition of atm., diss. and particulate halocarbons
- Atmospheric and dissolved other trace gases (CFCs, alkanes, etc.)
- DNA

WP Surface Microlayer
(PI Anja Engel)

- Dissolved and total organic carbon (DOC and TOC)
- Total nitrogen and total dissolved nitrogen (TN and TDN)
- CDOM, fluorescent DOM
- Total and dissolved combined carbohydrates
- Total and dissolved hydrolysable amino acids
- Bacterial cells number, phytoplankton cells number
- Marine gels (TEP, CSP)

WP DMS
(PI Cathleen Zindler)

- Underway and depths profiles of diss. DMS, diss./partic. DMSP, diss./partic. DMSO

WP Volatile Organic Compounds (VOCs) and oxygenated VOCs
(PI Jonathan Williams)

- Continuous atmospheric VOCs and OVOCs (methanol, acetone, DMS, isoprene, terpenes etc.)
- Atmospheric O_3
- Depth profiles of diss. VOC and OVOCs (isoprene, DMS, etc.)

WP Reactive Halogen Species
(PI Ulrich Platt)

- Atmospheric IO, BrO, NO_2, O_3, O_4, formaldehyde, glyoxal
- Atmospheric O_3

WP Air-sea Exchange and CO_2 Fluxes
(PIs Bernd Jähne, Christopher Zappa)

- Local heat transfer velocities

- Sea surface roughness (mean square slope), wave heights, wave frequency spectra
- Measurements of 2D slope, height maps of the sea surface, wavenumber/frequency spectra of waves
- CO_2 eddy covariance fluxes

WP Aerosols
(PI Alex Baker)

- Aerosol bulk composition

WP Nitrogen Isotopes and N_2/Ar
(PI Mark Altabet)

- Dissolved inorganic N (DIN) isotopes: NO_3^- and NO_2^- $\delta^{15}N$ and $\delta^{18}O$, NH_4^+ $\delta^{15}N$ and dissolved organic N (DON) $\delta^{15}N$
- N_2/Ar and $\delta^{15}N_2$
- N_2O: $\delta^{15}N$ and $\delta^{18}O$, and ^{15}N site preference
- Near-surface POM $\delta^{15}N$

3.3 Modification of the original proposal

The originally proposed WP by Jeff Hare had to be replaced with the WP by Bernd Jähne/Christopher Zappa because Jeff Hare moved from U Colorado to U Hawaii and was no longer interested in participation. Christa Marandino and Doug Wallace withdrew from the cruise because their instruments were not ready for the cruise (please note that the ship time was shifted forward to December 2012; the requested time window had been Spring 2013). The two vacant berths were given to the WP of Jonathan Williams and Birgit Quack. Because the second berth of the DWD was not occupied during M91 it was given to the WP of Mark Altabet.

3.4 Cruise track

Eight transects perpendicular to the coast and located between 5°S and 16°S have been sampled (A-E, G, I-J), see Figure 3.1 with cruise track below. They were identical to the regularly occupied oceanographic sampling lines of the Instituto del Mar del Peru (IMARPE, Callao, Peru) and cover the major upwelling centres along the coast of Peru. In addition we sampled the coastal time series stations off Callao (transect F) and a transect parallel to the Peruvian coast south of Callao (transect H). Transect H was chosen to sample the region where the anoxic event during M77/3 has been observed. The originally planned southern transect K (at ~17°S) was not sampled because of severe time constraints (the originally requested ship time had been cut by two days). Nevertheless, we were able to add one additional 24h station, thus, we had five instead of four 24h stations (for the positions of the 24h stations see Figure 3.1 below). Moreover, zodiac trips for surface microlayer sampling were added to our station planning (only during daylight stations). Four additional CTD/RO stations have been inserted (forming transect Ia) in the original station plan to sample the anticyclonic eddy which was detected already during M90.

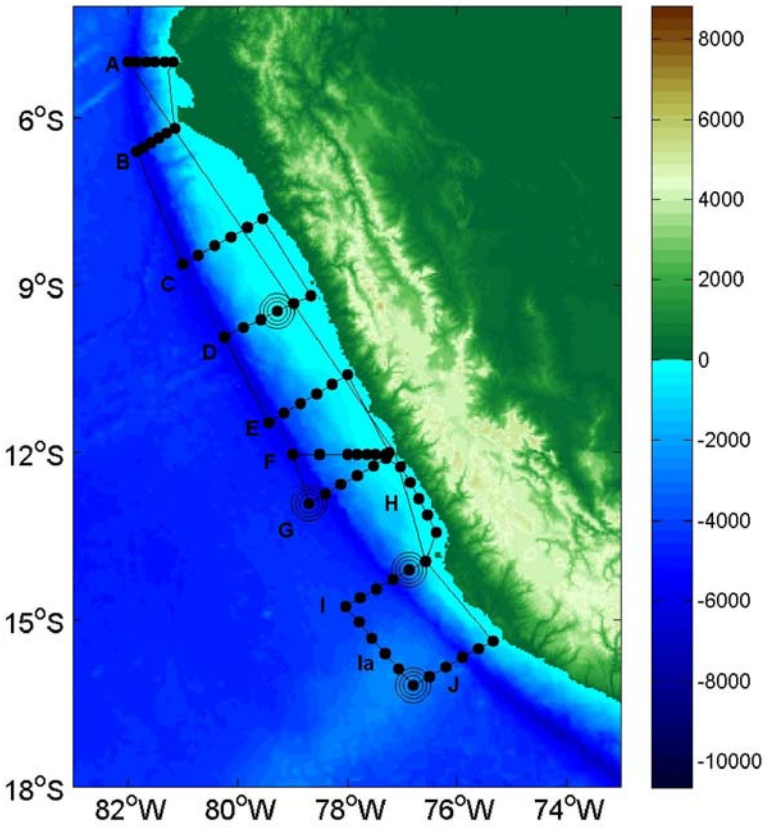

Fig. 3.1 Cruise track with locations of stations (black dots) of Meteor M91. Transects A-J are indicated as well as the locations of the 24h station (circles)

4 Narrative of the Cruise

Meteor left the port of Callao on 1 Dec 2012. After steaming north for one day, a CTD/RO test station was performed at 09° 3.61' S, 79° 58.82' W on 02 Dec. 2012. The first W/E transect at 5°S was reached on 3 Dec 2012 where the regular station work began. Each station usually consisted of one or two CTD/RO casts followed by a microstructure cast and sampling with the zodiac. A series of transects perpendicular to the coast were occupied while moving from north towards south. In total nine W/E transects (A-G, I, J) and two N/S transects (H and Ia), parallel to the coast, were occupied (see Figure 3.1 above). Additional to the regular sampling stations, five 24h-stations were performed during the transects D, G, I and J (see Figure 3.1 above). The work program of the 24h-stations in general included four CTD casts, four microstructure casts and several zodiac sampling trips. The anticyclonic eddy located off the coast and centred at about 16°30’S, 76°30’W, which was sampled by Lothar Stramma during the Meteor cruise M90 (Nov. 2012) as well, was sampled during the transects Ia and J from 20 to 23 Dec 2012. Station work was finished on 23 Dec in the evening. After the last station at 15° 22.76' S, 75° 19.91' W Meteor headed towards Callao, where the cruise M91 was finished in the morning of 26 December 2012. In total 98 CTD/RO stations, 55 microstructure casts and 45 sampling trips with the zodiac were performed. Moreover, continuous underway atmospheric and surface ocean sampling and measurements were performed along the entire cruise track.

5 Preliminary Results

5.1 CTD and Oxygen Measurements and Calibration

(T. Fischer, M. Krüger, T. Baustian, K. Rother)

During M91 98 profiles of pressure (p), temperature (T), conductivity (C) and oxygen (O_2) were recorded. These CTD-O_2 profiles usually ranged to 2000 m, where water was deep enough. When additional sample water was needed, a second CTD cast at the same place was conducted which usually ranged to 200 m. We used a Seabird Electronics (SBE) 9plus system (IFM-GEOMAR Kiel SBE-5), attached to the water sampler rosette, and the latest Seabird Seasave software. SBE-5 had two sensor sets: p #61184, T(1) #4673, C(1) #3366, O_2(1) #1314, T(2) #2814, C(2) #2512, O_2(2) #194. For the primary oxygen sensor being slightly noisier, the secondary sensor set was chosen for report. Conductivity was calibrated using a linear relation in p, T and C. This relation was obtained by fitting the CTD salinity to the best 66% (this level is usually chosen in order to remove obvious bad values) 170 corresponding bottle samples, which were analysed with a Guildline Autosal salinometer (#8). Root mean square (rms) salinity misfit of the resulting relation was 0.0008. O_2 was calibrated using a linear relation in p, T and O_2. Winkler titration of 1200 bottle samples led to a relation with a rms misfit of 0.6 µmol kg^{-1} (as well using the best 66% of bottle values). Further sensors were attached to the rosette and recorded during the majority of profiles, but were not calibrated: a fluorescence and turbidity sensor (Wetlabs #2294), a third oxygen sensor (Rinko #054), and a Photosynthetically Active Radiation (PAR) sensor (Biospherical #4702). An altimeter (Benthos #42106) permanently detected the CTD's distance to the bottom.

A particular feature of the shelf waters could be detected well in some CTD profiles: internal gravity waves of very high amplitudes compared to the water depth. These lead to sometimes extreme differences between the CTD downcast and upcast profiles. One example is shown in Figure 5.1. The possibility of such differences has to be kept in mind when comparing reported CTD profiles (that stem from downcasts) and water sample/bottle data (that stem from upcasts).

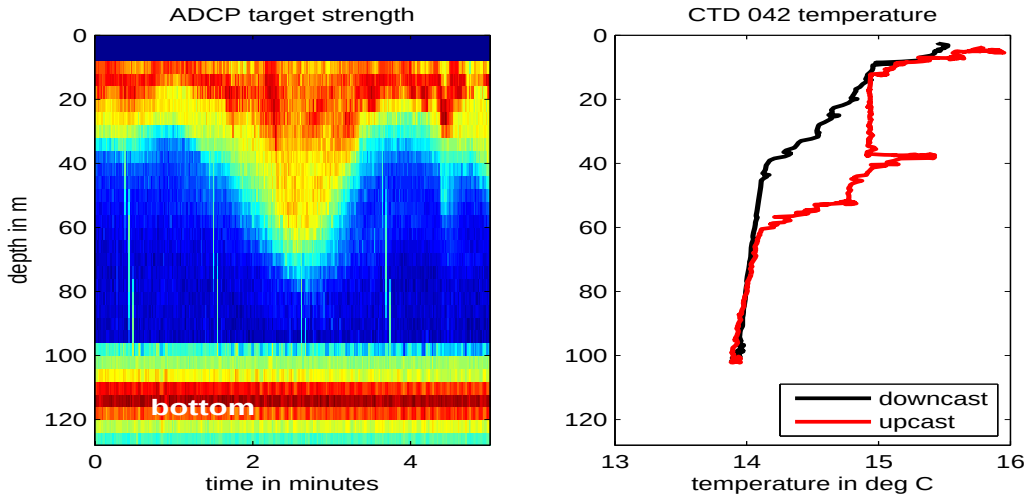

Fig. 5.1 A passing-by internal gravity wave producing pronounced differences between downcast and upcast CTD profiles. The backscatter of the 75 kHz ADCP (left panel) stems from an internal gravity wave comparable to the one that distorted the CTD profile 042 (right panel).

5.2 Current Observations

(T. Fischer)

Two vessel mounted Acoustic Doppler Current Profilers (ADCP) continuously recorded current velocities: a 75 kHz RDI Ocean Surveyor (OS75) mounted in the ship's hull, and a 38 kHz RDI Ocean Surveyor (OS38) placed in the moon pool. The OS38 was aligned to zero degrees in order to reduce interference with the OS75 that is aligned to a fix 45 degrees. Each of the two instruments was run in two configurations: one configuration in broadband mode (BB) for the shallower regions on the shelf and at the continental slope, and one configuration in narrowband mode (NB) for the deeper regions of the continental slope and the open ocean. The main reason to choose the less robust BB mode on the shelf was the higher possible resolution in space and time. The two configurations of OS75 were: a) NB mode, 100 bins of 8 m, pinging at 25 per minute, range 700 m; b) BB mode, 60 bins of 4 m, pinging at 60 per minute, range 250 m. The two configurations of OS38 were: a) NB mode, 55 bins of 32 m, pinging at 20 per minute, range 1300 m; b) BB mode, 80 bins of 16 m, pinging at 25 per minute, range 1000 m. During the entire cruise the SEAPATH navigation data were of high quality. Acoustic interference from other shipboard acoustic devices was avoided by switching these off whenever possible, particularly the Doppler Log and the multibeam echosounder. One exception was the 12 kHz echosounder EM122 which continuously delivered high quality bathymetry without detectable interference. A remaining source of noise was the bow thruster during stations.

Due to the extremely low oxygen concentrations in parts of the cruise area, there occurred patches and layers with extremely low abundance of acoustic scatterers. These low abundances sometimes caused a lack of interpretable acoustic backscatter signal (Figure 5.2), even when using the more robust NB mode.

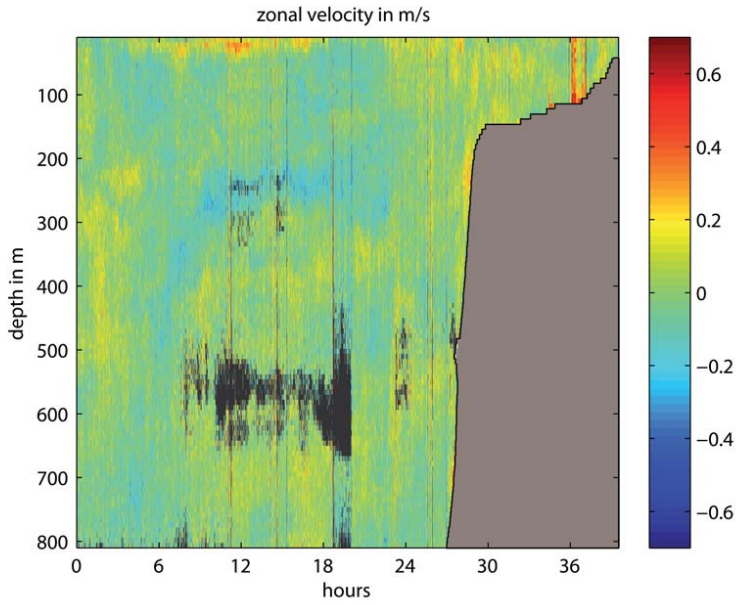

Fig. 5.2 Zonal velocity near the continental slope, exhibiting data loss from too low backscatter (black). The used 75 kHz Ocean Surveyor worked in narrowband mode. Ocean bottom is shaded grey.

5.3 Shipboard Microstructure Measurements

(T. Fischer)

A MSS90-D microstructure profiler (#032) of Sea and Sun Technology was used to infer turbulent dissipation rate and diapycnal diffusivity, particularly aiming at quantifying diapycnal fluxes of nitrous oxide (N_2O) in the Peruvian upwelling. The loosely tethered profiler was equipped with 3 airfoil shear sensors and a fast thermistor, as well as with a pressure, a conductivity, a temperature and a turbidity sensor. Profiler sink velocity was adjusted to 0.55 m/s. In total 170 profiles to maximum 500 m depth were recorded at 40 ship stations, generally 3 microstructure profiles following a CTD cast with N_2O sampling. Particularly at the continental rise and the shelf break we observed bottom intensified turbulence (one example profile is given in Figure 5.3), presumably caused by internal tides.

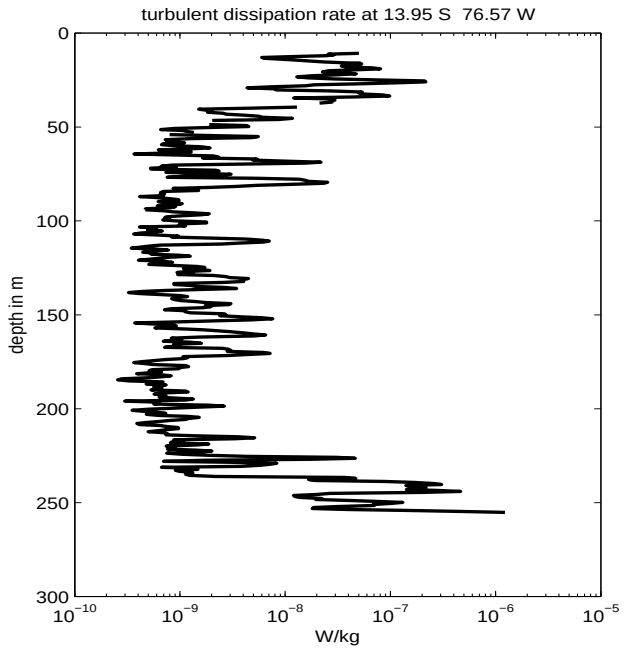

Fig. 5.3: Dissipation rate of turbulent kinetic energy, a measure of mixing intensity, at the shelf break at 260m water depth. The dissipation rate near the bottom is two orders of magnitude larger than in the water column above.

5.4 Upwelling Velocity

(Maike Peters, Reiner Steinfeldt, Jürgen Sültenfuß, Monika Rhein)

5.4.1 Scientific background

Coastal upwelling regions such as found in the research area of the Meteor cruise M91 off Peru belong to the most productive regions of the world ocean. Oceanic upwelling velocities, however, are too small to be measured directly. We, thus, make use of the deviations of the measured helium-3/helium-4 ratio from the expected ratio based on the equilibrium with the atmosphere to infer the vertical velocities. This method has already been applied in upwelling of the equatorial eastern Atlantic Ocean and the coastal region off Mauritania. The resulting vertical

velocities will be compared with Ekman theory. In conjunction with other measurements performed during M91, the upwelling velocities can be used to estimate the advective transport of heat, nutrients and trace gases into the mixed layer. Measurements of the samples and evaluation of the helium data will be done in the framework of the phase III of the BMBF project SOPRAN.

5.4.2 Parameters Sampled

384 helium samples in copper tubes have been taken from the Niskin bottles. Sampling focused on the mixed layer and the upper 200 m of the water column. The aim of the sampling strategy was to minimize the error of the mixed layer concentration of helium-3 and to get mean values of the helium-3 concentration and gradient below the surface in order to estimate the advective and diffusive input of helium-3 into the mixed layer.

5.4.3 Methods to be Used

In a first step, the gas has to be extracted from the water stored in the copper tubes, and this gas will then be transferred to a high resolution mass spectrometer. In addition to the helium isotopes helium-3 and helium-4, also the neon concentrations of the water samples will be analysed.

5.4.4 Time Line

The extraction, measurement and quality control of the helium samples will be done during the next year. The final data will be made available until the end of 2013.

5.5 Dissolved Oxygen and Hydrogen Sulphide Measurements

(Tina Baustian, Violeta Leon)

Samples for the determination of dissolved oxygen after Winkler (1888) were taken to calibrate the CTD´s oxygen sensors (SBE 43) and to support chemical and biological CTD data. Samples were collected from every hydrocast conducted during M91, except for those on stations M910/1720-1 and M910/1723-1, yielding a total of 94 collected casts. On a regular CTD cast, 5 to 23 depths between surface (3 – 5 m) and down to 2000 m (depending on the water depth) were sampled for dissolved oxygen. Additionally, dissolved oxygen samples were collected on 2 casts deeper than 2000 m (deepest cast down to 5000 m), yielding a total of 1217 samples for the entire cruise. To determine the precision of the oxygen concentration measurements determined from the titration, triplicate samples were taken for 1 to 2 depths at every station, yielding a total of 120 triplicates.

On two stations (M910/1758-1 and ME1766-3) an H_2S smell coming from the water samples indicated an anoxic event. Here, samples for the analysis of H_2S were collected from the respective water samples instead of (Stn M910/1758-1) or in parallel to (Stn M910/1766-3) the oxygen samples and analysed for H_2S using the titration method after Andersen and Foyn (1969).

5.6 Dissolved Nutrients

(Kerstin Nachtigall)

Nutrients were measured on-board with a QuAAtroAutoanalyzer from SEAL Analytical. The following methods from SEAL analytics were used:

Nitrite and Nitrate – Q-068-05 Rev 7; The nitrate is determined as nitrite after reduction on a cadmium coil. The nitrite is determined with a colorimetric method where sulphanilamide is forming a diazo compound.

Phosphate – Q-064-05 Rev 4; this is the colorimetric method based on reaction with molybdate and antimony ions.

Silicate – Q-066-05 Rev 3; this is the colorimetric method where a silico-molybdate complex is reduced to molybdenum blue.

Samples from the CTD were measured on every CDT cast yielding a total of 1275 samples during the cruise. The precision of the nutrient measurements were determined from triplicate samples taken at selected stations. The precisions of the measurements, given as the mean standard deviation of all triplicate samples, were: ± 0.09 µmol L^{-1} for nitrate, ± 0.02 µmol L^{-1} for phosphate, ± 0.01 µmol L^{-1} for nitrite and ± 0.06 µmol L^{-1} for silicate.

Ammonia was determined after Holmes et al. (1999) using a fluorometer. 295 duplicate samples were taken from the CTD stations with water depth less than 700 m. The precision of the measurements was ± 0.03 µmol L^{-1}.

In addition to the CTD casts, nutrient samples were analysed from underway measurements.

5.7 Phytoplankton, Coccolithophorids Diversity, DIC, Total Alkalinity, pH, Chlorophyll a

(Violeta León, Georgina Flores, Avy Bernales, Michelle Graco)

5.7.1 Methods

The CTD-rosette measurement and sampling program of IMARPE included (1) pH and Chlorophyll-a collected from all depth profiles and (2) total alkalinity (TA), dissolved inorganic carbon (DIC) as well as Ca and Si isotopes during the transect F (off Callao). In order to compare the nutrient method from IMARPE with the method from GEOMAR we took samples for nutrients from one profile in transect (G). Also, our group worked together with other working groups on board by taking samples and making measurements of dissolved oxygen, ammonium, nutrients, nitrous oxide, dimethyl sulphide (DMS) and DNA filtrations.

5.7.1.1 Phytoplankton Quantitative Analysis by Utermöhl Method

Phytoplankton samples were taken from 3 m to 75 m parallel to the DMS measurements during the Chimbote and Callao transects (transects B and F, respectively), These samples will be analysed in the phytoplankton laboratory at IMARPE to determine potential DMS producing phytoplankton species.

5.7.1.2 Determination of Coccolithophorids Diversity

Two litres of seawater were sampled by filtrating with a net (15 µm mesh size) along the coast and offshore stations during the Chimbote and Callao transects (transects B and F, respectively) to determine the diversity of coccolithophorids. All samples were fixed with neutralized formaldehyde (20 %).

5.7.1.3 Method using Sedgewick-Rafter Cell for Red Tides Counts

A Sedgewick-Rafter cell is widely used for the quantification of phytoplankton with a volume of 1 mL (50 mm length x 20 mm width x 1 mm height). The bottom plate of the Sedgewick-Rafter cell is divided into 50 columns and 20 rows forming 1000 squares altogether.

5.7.1.4 DIC and TA Sampling Procedures

Glass sample bottles were filled smoothly from the bottom by using a tube connected to the Niskin bottle at the CTD/Rosette. Saturated aqueous mercuric chloride ($HgCl_2$) solution was added to poison the sample. The samples were stored cooled in the dark until the measurements. The DIC samples will be measured by using a non-dispersive infrared analyser from LI-COR Biosciences. Alkalinity will be measured with a METROHM automatic titrator.

5.7.1.5 pH

pH was determined by applying the method of Dickson with a Mettler Toledo Potentiometer which was equipped with a glass/reference electrode cell. Samples were taken from all transects. About 1000 samples for pH were measured along transects.

5.7.1.6 Chlorophyll-a

Chlorophyll-a was measured on-board with a Trilogy® Laboratory Fluorometer (Turner Designs) by applying the method of Holm-Hansen.

5.7.2 Time line

Values of chlorophyll will be calculated as soon as we have received the calibration factor of the Fluorometer. DIC and TA measurements will performed by the State Key Laboratory of Marine Environmental Science of the Xiamen University in China. The measurements of nutrients, coccolithophorids diversity and the quantitative phytoplankton analysis will be performed at IMARPE. The results will be available in July 2013.

5.8 DMS, DMSP and DMSO Measurements

(Verena Ihnenfeld, Avy Bernales, Cathleen Zindler, Hermann Bange)

5.8.1 Scientific Background

Dimethyl sulphide (DMS), dimethyl sulphoniopropionate (DMSP) and dimethyl sulphoxide (DMSO) are key players in the marine sulphur cycle and the microbial foodweb (Simó, 2001). The DMS emissions from the ocean account for about 40 % of the sulphur compounds in the atmosphere (Charlson et al., 1987).

In order to acquire more information about these sulphur compounds the concentrations of DMS, particulate DMSP ($DMSP_p$), dissolved DMSP ($DMSP_d$), particulate DMSO ($DMSO_p$) and dissolved DMSO ($DMSO_d$) were determined in the Peruvian upwelling region. Furthermore, a comparison of the distribution of DMS and DMSP concentrations with the phytoplankton composition and its density might deliver important information as DMSP is one of the products of primary production. Moreover the DMS flux from the ocean into the atmosphere from the upwelling off Peru will be quantified. We will compare our measurements with the DMS measurements by Patrick Veres and Bettina Derstroff (MPI Mainz) during M91. In addition to that a comparison of the results with measurements from the Mauritanian upwelling may give a better insight into the sulphur cycle in coastal upwelling systems.

5.8.2 Parameters Measured and/or Sampled

Additional to sampling for DMS/DMSP/DMSO from selected depth profiles, underway surface seawater samples were taken every 6 hours except when the ship was on station (see Tab. 5.8).

Tab. 5.8: List of underway samples (sampling time is given in UTC).

UW No.	Date/Time (UTC)	UW No.	Date/Time (UTC)	UW No.	Date/Time (UTC)
1	3.12.12/5h	**15**	6.12.12/11h	**33**	10.12.12/23h
2	3.12.12/11h	**17**	6.12.12/23h	**35**	11.12.12/5h
3	3.12.12/17h	**18**	7.12.12/5h	**37**	11.12.12/11h
4	3.12.12/23h	**19**	7.12.12/11h		
5	4.12.12/5h	**20**	7.12.12/17h		
6	4.12.12/11h	**21**	7.12.12/23h		
7	4.12.12/23h	**23**	9.12.12/11h		
9	5.12.12/5h	**24**	9.12.12/17h		
10	5.12.12/11h	**26**	9.12.12/23h		
11	5.12.12/17h	**27**	10.12.12/5h		
12	5.12.12/23h	**29**	10.12.12/11h		
13	6.12.12/5h	**30**	10.12.12/17h		

5.8.3 Methods Used/to be Used

DMS was measured on board using a Gas Chromatograph (GC)/Flame Photometric Detector (FPD) system. 250 ml seawater was taken from the CTD/Rosette. For the determination of DMS filtrated (GF/F Filter) triplicates (each 10 ml) were directly measured after sampling. For the determination of $DMSP_d$ filtrated triplicates of sampled seawater (each 10 ml) were alkalized with NaOH pellets in order to convert DMSP into DMS and stored until the measurements were conducted. For determination of $DMSP_p$ 50 ml unfiltrated sample water was alkalized and measured not later than 24 h after sampling. For the determination of DMSO/DMSO cobalt-doped sodium borohydride ($NaBH_4$) pellets were added to filtrated (for the determination of $DMSO_d$ and not filtrated (for $DMSO_p$) triplicates of sampled seawater (each 10 ml) in order to convert the DMSO into DMS.

In order to expel DMS out of the seawater, the seawater samples were purged with helium (He). Gaseous DMS was transported with the helium gas stream into a trap consisting of a Teflon tube submerged into liquid nitrogen in order to preconcentrate DMS. The gas stream was dried using potassium carbonate. After purging the trap was heated up and the DMS was transferred onto the gas chromatography column where it was separated from other gaseous compound and detected with the FPD.

5.8.4 Preliminary Results

The measured DMS concentrations in the Peruvian upwelling region showed surface concentrations between 0.3 und 9.1 nmol L^{-1}. At the stations during the transect Ia comparably high DMS concentrations between 4.6 and 5.7 nmol L^{-1} were measured. In this region Patrick Veres and Bettina Derstroff (MPI Mainz) measured elevated DMS concentrations in the air. This leads to the assumption that the regional anticyclonic eddy caused the high DMS concentrations and represents a pronounced source of DMS in the atmosphere. In addition to that the DMS concentrations during the transect F off Callao were elevated, which may have been caused by a strong anthropogenic influence by the cities of Lima and Callao.

The depth profiles showed subsurface maxima at different depths for all measured parameters. At depths deeper than 75 m the DMS concentration was too low to be measured. DMSO could be found all through the water column. The Figures 5.8-1 and 5.8-2 show representative depth profiles of all measured parameters: DMS, DMSP (dissolved and particulate) and DMSO (dissolved and particulate).

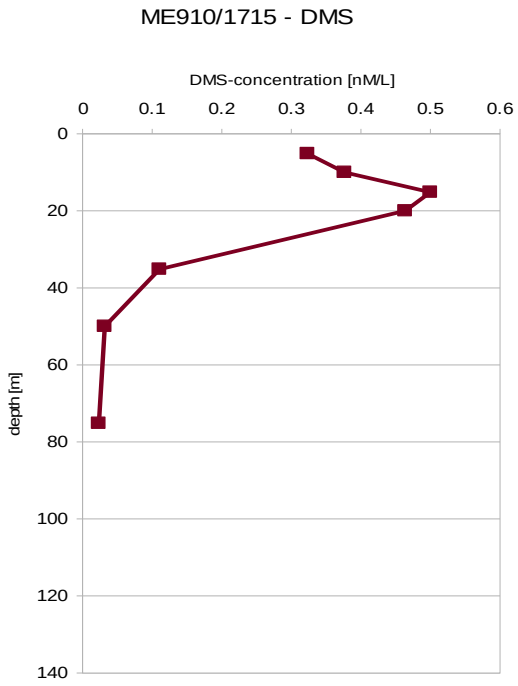

Fig. 5.8-1: DMS depth profile at M910/1715

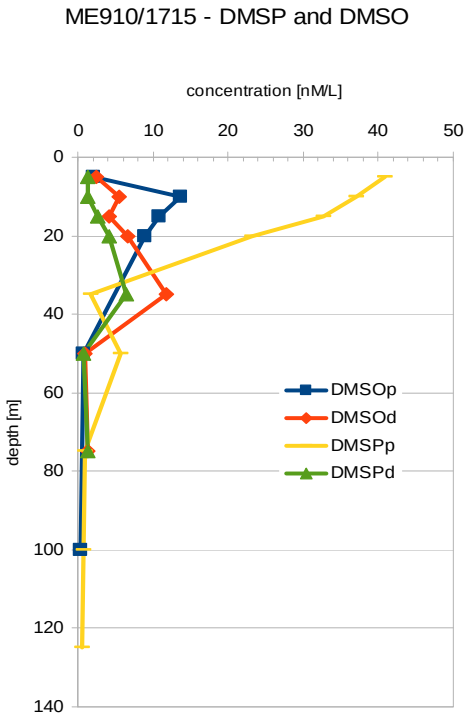

Fig. 5.8.-2: DMSP and DMSO depth profiles.

5.8.5 Time Line

The remaining samples for DMSP and DMSO will be measured after the cruise in the home lab at GEOMAR. The final data set will be available by December 2013.

5.9 Dissolved and Atmospheric Halocarbons, Halogens, Radio Sounding and Disdrometer, Phytoplankton Pigments, Flow Cytometry, DNA Filtration

(Helmke Hepach, Sebastian Flöter, Stefan Raimund, Birgit Quack, Steffen Fuhlbrügge, Kirstin Krüger, Elliot Atlas, Avy Bernales, Harald Biester, Astrid Bracher, Christa Marandino)

5.9.1 Scientific background

Halogenated hydrocarbons (halocarbons) occur naturally in the oceans. They take part in numerous chemical processes such as ozone chemistry in both troposphere and stratosphere and participate in aerosol formation (Vogt et al., 1999; Salawitch et al., 2005; O'Dowd et al., 2002). Especially coastal regions with high macroalgal abundance are characterized by elevated concentrations of halocarbons (Carpenter and Liss, 2000; Laturnus, 2001) but upwelling areas with high primary production via phytoplankton are potential source regions as well (Quack et al., 2007a; Quack et al., 2007b). Bromoform ($CHBr_3$) and dibromomethane (CH_2Br_2) in particular are most likely of biological origin and represent the largest contributors to atmospheric organic bromine from the ocean to the atmosphere (Hossaini et al., 2012). Thus, the biological active Peruvian upwelling could be a potential source region for these brominated trace gases. In contrast to this, methyl iodide (CH_3I) may be rather a product of photochemical

processes taking place in the surface ocean (Richter and Wallace, 2004), being thus more connected to parameters such as insolation and sea surface temperature (SST).

During the DRIVE (Diurnal and RegIonal Variation of halogen Emissions) campaign in June 2010 (Poseidon cruise P399), which took place in the Mauritanian upwelling, high concentrations of CH_2Br_2 and $CHBr_3$ were found in the surface water close to and in the upwelling. These were also associated with high atmospheric halocarbon concentrations caused by an inverse relationship of atmospheric halocarbons with the height of the Marine Atmospheric Boundary Layer (MABL) (Fuhlbrügge et al., 2012): higher heights, associated with warmer oligotrophic waters, were accompanied by lower atmospheric halocarbons, while lower heights due to the lower SST of the upwelling water were connected to higher atmospheric abundances of these trace gases. This also has a potential suppressing effect on emissions of halocarbons from the upwelling (Hepach et al., 2013). During M91, we try to verify this phenomenon in the upwelling off Peru which seems to be comparable to the Mauritanian upwelling. This was done by parallel air and surface water sampling, as well as by radio sonde launches for the determination of MABL heights. There is also still large uncertainty with regard to production of halocarbons and their general fate in the water column. This was investigated by parallel sampling of halocarbons, phytoplankton pigments, iodide and iodate and particulate organic bromine (POBr) and iodine (POI) from water profiles and the ship's underway pump system. Additionally, a possible relationship of DMS to CH_3I was explored with parallel sampling of depth profiles for both compounds, as well as filtration for DNA.

5.9.2 Parameters Measured and Sampled

5.9.2.1 Underway Measurements of Dissolved Compounds

	Parameter	Method
Halocarbons	CH_3I, $CH_2Cl_2CHCl_3$, CCl_4, CH_3CCl_3, CH_2Br_2, CH_2ClI, $CHBr_2Cl$, CH_2BrI, $CHBr_3$, CH_2I_2	Purge and Trap with GC-MS / GC-ECD
Phytoplankton pigments	Chlorophyll a, Divinyl Chlorophyll a, Chlorophyll b, Divinyl Chlorophyll b, Chlorophyll c1+2, Chlorophyll c3, Peridinin, 19-butanoyl-oxy-fucoxanthin, Fucoxanthin, Neoxanthin, 19-hexanoyl-oxy-fucoxanthin, Violaxanthin, Diadinoxanthin, Antheraxanthin, Alloxanthin, Diatoxanthin, Zeaxanthin, alpha Carotene, beta Carotene	Filtration and HPLC
Phytoplankton identification	Nanoplankton, Picoplankton, Prochlorococcus, Synechococcus	Flow cytometry
Ox/red inorg. halogens	I^-, IO_3^-, Br^-, Br_3^-	Filtration
Particulate org. halogens	POBr, POI	Filtration

5.9.2.1.1 Sampling Frequency

- Halocarbons: every 3 h (0, 3, 6, 9, 12, 15, 18, 21 LT)
- Phytoplankton pigments and flow cytometry: approximately every 6 h (12, 18, 0 LT)
- Oxygenated and reduced halogens: approximately every 12 h (12, 0 LT)
- Particulate organic halogens: approximately once every 24 h (12 LT)

5.9.2.2 Underway Measurements of Atmospheric Trace Gases, Radio Sounding and Disdrometer

5.9.2.2.1 Parameters to be Analysed in the Discrete Air Samples (Canisters)

CH_2Br_2, $CHClBr_2$, $CHBr_3$, F-12, F-11, F-113, F-114, F-22, F-142b, F-141b, HCFC-124, F-134a, HFC-152a, F-12b1, F-114b2, DMS, COS, Propane, n-Butane, i-Pentane, n-Pentane, n-Hexane, Isoprene, Benzene, Toluene, CH_3Cl, CH_3Br, CH_3I, CH_2Cl_2, $CHCl_3$, 1,2-Dichloroethane, CH_3CCl_3, CCl_4, C_2Cl_4, $MeONO_2$, $EthONO_2$, i-$PropONO_2$, n-$PropONO_2$, 2-$ButylONO_2$, Methyl acetate.

5.9.2.2.2 Parameters Sampled with Radio Sounding and Disdrometer

- Air temperature (radio sounding)
- Wind speed and – direction (radio sounding)
- Humidity (radio sounding)
- Rain rate (disdrometer)
- Drop size (disdrometer)
- Rain amount (disdrometer)

5.9.2.2.3 Sampling Frequency

Air sampling:	*Start*	*End*
6 hourly:	01.12.2012 23 UTC	03.12.2012 05 UTC
3 hourly:	03.12.2012 08 UTC	14.12.2012 11 UTC
	17.12.2012 08 UTC	18.12.2012 11 UTC
	20.12.2012 14 UTC	22.12.2012 23 UTC
	23.12.2012 17 UTC	23.12.2012 23 UTC
	24.12.2012 05 UTC	24.12.2012 08 UTC
2 hourly	14.12.2012 13 UTC	17.12.2012 05 UTC
	18.12.2012 13 UTC	20.12.2012 11 UTC
	24.12.2012 01 UTC	24.12.2012 03 UTC
	24.12.2012 15 UTC	24.12.2012 21 UTC
2 samples / 3 hours	23.12.2012 01 UTC	23.12.2012 14 UTC

Radiosondes:		
6 hourly	02.12.2012 00 UTC	02.12.2012 12 UTC
	03.12.2012 00 UTC	03.12.2012 12 UTC
	04.12.2012 00 UTC	04.12.2012 06 UTC
	05.12.2012 06 UTC	07.12.2012 00 UTC
	09.12.2012 06 UTC	11.12.2012 06 UTC
	12.12.2012 06 UTC	12.12.2012 12 UTC
	13.12.2012 06 UTC	13.12.2012 12 UTC
	14.12.2012 18 UTC	15.12.2012 06 UTC
	19.12.2012 00 UTC	20.12.2012 12 UTC
	22.12.2012 00 UTC	22.12.2012 18 UTC
3 hourly	02.12.2012 15 UTC	02.12.2012 18 UTC
	03.12.2012 15 UTC	03.12.2012 21 UTC
	08.12.2012 00 UTC	09.12.2012 00 UTC
	12.12.2012 15 UTC	13.12.2012 00 UTC
	13.12.2012 15 UTC	14.12.2012 12 UTC
	17.12.2012 09 UTC	18.12.2012 18 UTC
	20.12.2012 15 UTC	21.12.2012 18 UTC
	21.12.2012 21 UTC	23.12.2012 18 UTC

5.9.2.3 CTD Measurements / Depth profiles

- Halocarbons
- Phytoplankton pigments and flow cytometry
- Oxygenated and reduced halogens
- DNA filtration

5.9.3 Methods used/to be used

5.9.3.1 Halocarbon Determination

Dissolved halocarbons in sea water were determined from underway measurements and depth profiles using two purge-and-trap-systems equipped to combined gas chromatography and mass spectrometry (GC-MS), as well as to a gas chromatograph equipped with an electron capture detector (GC-ECD). Water samples were taken in 300 ml amber glass bottles. In the purge and trap system attached to the GC-MS, 50 ml of water were purged. In the purge and trap system attached to the GC-ECD, 30 ml of sampled water were purged. After 40 – 60 min of purging, the sample was analysed for halocarbons. For a detailed description of the purge and trap systems see Hepach et al. (2013). Volumetrically prepared standards in methanol were used for quantification.

Air samples were taken in stainless steel canisters on the ships' compass deck using a metal bellows pump attached to a stainless steel sampling line. Samples will be shipped to the Rosenstiel School of Marine and Atmospheric Science (RSMAS) in Miami where they will be analysed by the group of Elliot Atlas according to Schauffler et al. (1999).

5.9.3.2 Radio Sounding and Disdrometer

The radiosondes (type: RS92-SGP) were used to measure temperature, humidity, wind speed and – direction from the surface up to about 25 km height. As long as the ship was at least 25 nm away from the coast, the radiosondes were launched - with assistance of the German Weather Service (DWD) - 4 times a day at 00, 06, 12 and 18 UTC and also at 03, 09, 15 and 21 UTC at the 24 h stations. The resulting profiles are further used to determine the height of the atmospheric boundary layer at each ascent. This parameter indicates the vertical extension of mixing within the lower troposphere, usually from the ground up to 1 – 3 km height. The optical disdrometer 'ODM 470' takes continuous precipitation measurements, containing rain rate, drop size and amount but also wind speed and direction.

5.9.3.3 Phytoplankton Pigments and Flow Cytometry

Water samples for phytoplankton pigments and flow cytometry were taken both from the ship's underway pump system and from depth profiles. For determination of smaller plankton groups, 20 µL of 25 % glutardialdehyde were added to 4 mL of sampled sea water. After 15 min, they were frozen in liquid nitrogen and stored at -80 °C. Back in the lab at the AWI, samples will be analysed using flow cytometry. For pigment analysis, up to 2 L of sampling water were filtered onto 25 mm GF/F filters for not more than 60 min. Filters were than frozen in liquid nitrogen and stored at -80 °C. Back in the lab, filters will be analysed according to Hoffmann et al. (2006) using a high-performance liquid chromatography (HPLC) system.

5.9.3.4 Oxygenated and Reduced Halogens

50 mL of sea water from both the underway pump system and depth profiles were filtered into falcon tubes through Sarstedt Filtropur S 0.2 filters using a membrane pump for determination of iodide and iodate. Samples were then stored in the dark at -20 °C until analysis. They will be analysed at the TU Braunschweig using coupled HPLC-UV-ICPMS.

5.9.3.5 Particulate Organic Halogens

For POBr and POI, sea water was continuously pumped through Sartorius Stedim cellulose nitrate filters with a diameter of 14.2 cm and a pore size of 0.45 µm using a pump attached to the ship's underway pump system. The filtration was stopped after 4 – 8 h depending on the particle quantity on the filter. The material filtered onto the filters will be analysed at the lab at the TU Braunschweig using UV-vis detection for iodine and µ-XRF for bromine.

5.9.3.6 DNA Filtration

Water for determination of DNA was filtered no more than 20 min through Millipore membrane filters with a diameter of 47 mm. Samples were stored at -80 °C. Samples will be analysed at the lab in Kiel.

5.9.4 Preliminary Results

5.9.4.1 Surface Water Concentrations of Halocarbons

Due to contamination problems, underway measurements of halocarbons could only start 11December (transect E). Quantification of the halocarbon underway data has yet to be finalized. First evaluations of data show no particular halocarbon hot spots in the surface water so far. Concentrations of CH_2Br_2 and $CHBr_3$ were, especially in the southern parts of the cruise, rather low and only slightly elevated in comparison to common open ocean values. For $CHBr_3$, concentrations hardly ever reached more than 20 pmol L^{-1} which has previously been measured in other upwelling regions (Hepach et al., 2013). In the southern transects of the M91 cruise, rather low bioactivity could be observed as well. Similarly, CH_3I showed higher concentrations in the middle part of the cruise and low values in the southern transects.

Future evaluation will include comparison with air measurements, phytoplankton pigment data and oxygenated and reduced halogens. Halocarbon data will be compared to determined MABL heights.

5.9.4.2 Depth Profiles of Halocarbons

First results of halocarbon measurements in the water column show a distinct distribution with maxima in the mixed layer. Figure 5.9-1 shows the distribution of $CHBr_3$ in the water column at station 1774. Similar to all other measured halocarbons, $CHBr_3$ has its maximum in the first 50 m and decreases rapidly in the oxygen minimum zone. Similar depth profiles were obtained from about 25 other stations throughout the cruise.

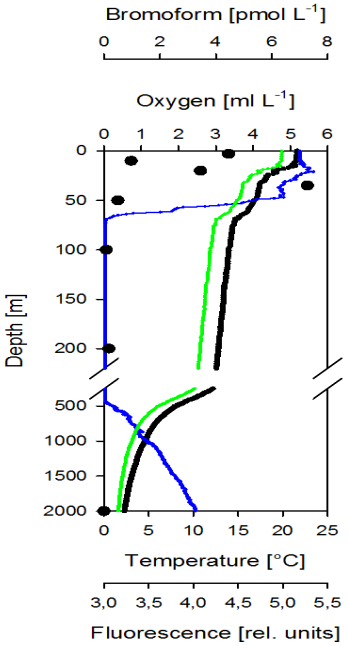

Fig 5.9-1. Depth profile of $CHBr_3$ (black dots), oxygen (blue line), temperature (black line) and fluorescence (green line) at station M910/1774.

5.9.4.3 Radiosoundings

The temperature profiles (Figure 5.9-2) reveal a tropopause height of about 16 – 18 km height, which is typical for tropical regions. We also have trade inversions between 1 and 2 km height. The -very preliminary- boundary layer height is found between 0.5 and 1 km, in most cases limited by the trade inversions. The measurements indicate surface inversions up to 100 m that might influence and reduce the boundary layer height, too. However, the humidity profiles (Figure 5.9-2) reflect a good mixing of water vapour up to the base of the trade inversions. In addition a change of wind direction and speed is observed at these inversions, with a decrease of southern and an increase of the western wind component above the inversions.

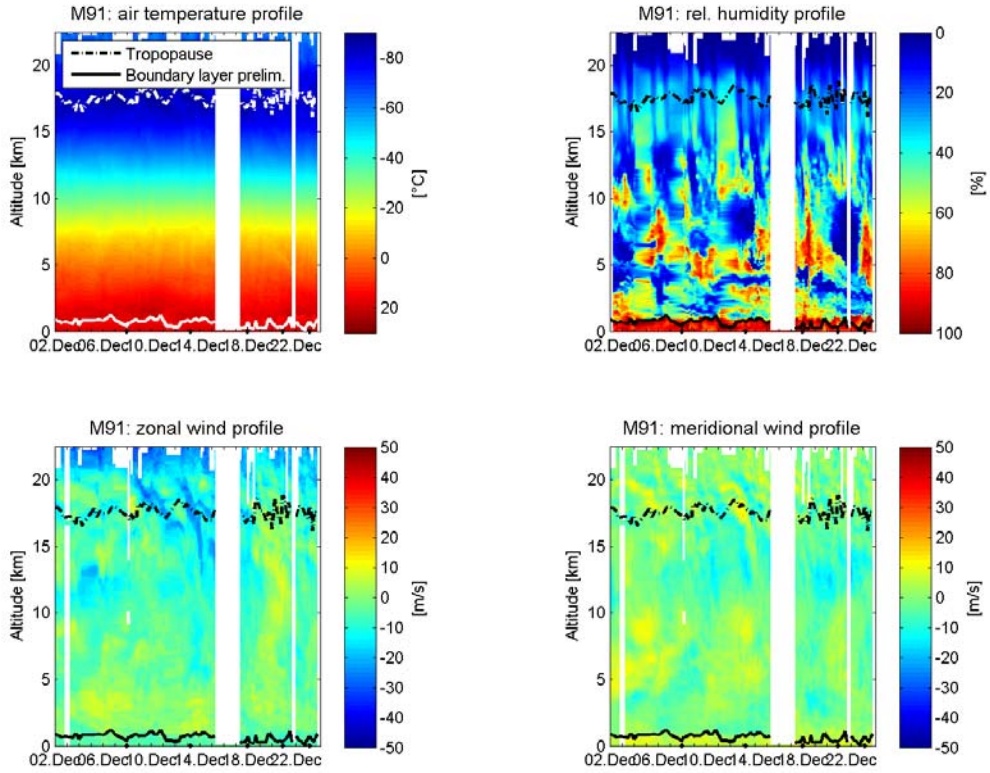

Fig. 5.9-2. First results from radio sounding measurements (upper row: air temperature and relative humidity, lower row: zonal and meridional wind profiles).

5.9.5 Time Line

5.9.5.1 Halocarbon Measurements

All measurements of halocarbons in seawater were completed on-board the R/V Meteor. Final quantification will be available 6 months after the cruise. Analysis of air samples will take place at RSMAS in Miami. Analysis will be completed approximately 6 months after the cruise.

5.9.5.2 Radio sounding and Disdrometer

Final data from radio soundings and the disdrometer will be available approximately 2 months after the cruise.

5.9.5.3 Phytoplankton Pigments and Flow Cytometry

Analysis of frozen samples for phytoplankton pigments and flow cytometry will be performed at the AWI Bremerhaven. Analysis will probably take place in the next 6 months. Further work will include comparison to satellite data and calculation of species composition with Chemtax®.

5.9.5.4 Oxygenated and Reduced Halogens

On-board the R/V Meteor, samples were filtered and frozen. Analysis of the samples will take place at the TU Braunschweig in the next 6 months.

5.9.5.5 Particulate Organic Bromine and Particulate Organic Iodine

Filtering of samples took place on-board the RV Meteor after which they are frozen at -20 °C until analysis at the TU Braunschweig. Results will be available the latest in 6 months.

5.10 Isotope Composition of Halocarbons and Molecular Biological Analyses

(Ingo Weinberg, Richard Seifert, Detlef Schulz-Bull, Walter Michaelis, Falk Pollehne, Klaus Jürgens, Enno Bahlmann, Christian Stolle, Anna Orlikovska)

5.10.1 Scientific Background

Much progress in quantifying the global emissions of various volatile halogenated organic compounds (VHOCs) has been made within the last years. However, due to the inevitably large spatial and temporal variability in observed halocarbon mixing ratios and fluxes the current emission estimates in particular for CH_3I and $CHBr_3$ are still assigned with large uncertainties (Quack et al. 2004; Butler et al. 2007; Carpenter et al. 2008, O'Brien et al. 2009; Palmer & Reason 2009; Liang et al. 2010); this with the largest uncertainties existing with regard to coastal and near shore emissions (WMO 2010). An improved understanding of the underlying biogeochemical controls may substantially reduce these uncertainties and is of vital importance to address potential future changes. Primary production of marine algae has been assumed to provide the basic material for VHOCs emissions and macroalgae are known to be strong VHOCs producers (Gschwend et al. 1985, La Barre et al. 2010). Increasing evidence accumulated that diverse microalgae also contribute strongly to VHOCs production, such as small red algae (Collén et al. 1994), diatoms (Scarratt and Moore 1996) or cyanobacteria (Karlsson et al. 2008, Hughes et al. 2011). However, the regulation of the biological production / decomposition equilibrium of halogenated hydrocarbons and its relation to external factors like changes in the light- and nutrient-environment are not well understood.

Carbon isotope signatures of individual halocarbons emerged as a powerful tool to distinguish different sources, to obtain information on source and sink mechanisms, and to refine their global budgets (Mc Cauley et al. 1999; Harper et al. 2003; Keppler et al. 2005). In particular the $\delta^{13}C$ values of the monohalomethanes vary sensitively towards changes of both, sources and sinks, making them a valuable tool to assess the biogeochemical turnover. We aim to investigate the main sources and the processes controlling the production and decomposition of reactive trace gases in upwelling systems as well as their air-water exchange in comparison to the open ocean. A specific point of interest is biological turnover of VHOCs in the surface ocean with

emphasis on the distribution and diversity of functional enzymes in VHOCs degradation and production.

5.10.2 Measurements

A comprehensive set of samples (air, seawater, particulate matter) was secured for subsequent determination in the laboratories of the IfBM (Hamburg) and the IOW (Warnemünde). Air and water samples will be analysed for halocarbons such as CH_3Cl, CH_3Br, CH_3I, CH_2Br_2, $CHBr_3$ as well as CFCs, alkanes, oxygenated hydrocarbons, and sulphur-containing compounds. In order to determine the microbial/planktonic DNA, filtrations of water samples were performed. The majority of sampling (air and water) was performed underway. However, punctual water sampling was done station-based from various water depths.

5.10.3 Methods

A high-volume air sampling system was installed on the observation deck (air chemistry lab). About 300 L of ambient air were sampled three times a day (morning, midday, evening/darkness) in order to determine VOCs (Bahlmann et al. 2011).

Dissolved VOCs were processed using a Purge&Trap system which was operated in the sampling room (Abfüllraum). The 20 L water samples were basically taken from the pump (Lotschacht, depth: 5.60 m) or punctually from the CTD (3 bottles per CTD cast) with varying depths.

The VOCs from air and water samples were enriched on cryotraps submerged in a dry shipper filled with liquid nitrogen, transferred to sampling tubes, and stored at -80 °C until shipment (Bahlmann et al. 2011).

For the determination of microbial/planktonic DNA an aliquot per water sample was filtrated (0.2 µm filter). The filters were stored at -80 °C until shipment.

Stable carbon isotope ratios of VOCs will be determined using an isotope-ratio-mass-spectrometer at our home laboratories (IfBM and IOW) as well as the microbial work (IOW).

5.10.4 Time Line

All laboratory work including the determinations of stable isotope ratios is scheduled to be accomplished until the end of 2013.

5.11 Measurements of N_2O, CO, CO_2, CH_4 and short-lived N compounds

(Damian Arevalo Martinez, Joel Craig, Georgina Flores, Annette Kock Tobias Steinhoff, Hermann Bange)

5.11.1 Scientific Background

Nitrous oxide (N_2O), methane (CH_4) and carbon dioxide (CO_2) are long-lived greenhouse gases and the main contributors to the anthropogenic greenhouse effect. Carbon monoxide (CO) is a short-lived trace gas that plays an important role in tropospheric chemistry. Gas exchange with the ocean plays an important role in the cycling of these gases, and eastern boundary upwelling systems have been shown to be particularly important areas where nutrient-enriched waters are

brought to the surface ocean and initiate high primary production. The high biological productivity and the transport of subsurface waters that are enriched in trace gases to the surface ocean make these areas particularly interesting for studying the gas exchange of N_2O, CH_4, CO_2 and CO.

Measurements of N_2O, CH_4, pCO_2 and pCO during M91 were conducted to serve a number of different purposes:

- High resolution underway measurements of surface pN_2O, pCO and pCO_2 allow a detailed determination of the spatiotemporal distribution of these trace gases and the quantification of their air-sea gas exchange. Furthermore, combined underway measurements of pN_2O and pCO_2 allow the calculation of net community production according to Steinhoff et al. (2012).
- Depth profiles of N_2O were taken in coordination with microstructure profiles to determine the subsurface distribution of N_2O in the Peruvian upwelling and to allow the quantification of the flux of N_2O from the subsurface ocean to the mixed layer.
- High resolution profiles from the upper 10 m of the water column were taken during five zodiac deployments (stations 1733, 1752, 1761, 1764, 1777) to investigate a potential effect of a diurnal stratification within the mixed layer on N_2O saturations. Diurnal stratification of the upper few meters of the mixed layer had been observed during previous expeditions and gave room for speculations of the effect of short-term stratification on N_2O emissions from tropical areas.
- N_2O and CH_4 sampling from the Callao Time Series Transect (= Transect F during M91) was conducted to complement the regular time series sampling for N_2O and CH_4 conducted by the Instituto del Mar del Peru (IMARPE) in Callao as part of a collaboration between IMARPE and the SFB754 (www.sfb754.de).

5.11.2 Continuous pN_2O/pCO and pCO_2 measurements

An underway system was used to perform continuous measurements of oceanic and atmospheric nitrous oxide (N_2O), carbon monoxide (CO) and carbon dioxide (CO_2). It combines an OA-ICOS (off-axis integrated cavity output spectroscopy) analyser from Los Gatos Research Inc. for N_2O and CO, a non-dispersive infrared analyser from LI-COR Biosciences for CO_2 determinations and a Weiss type equilibrator. The water was drawn on board by using a submersible pump installed at the moonpool of the ship and was subsequently conducted at a rate of about 2 L min^{-1} through the equilibrator. Air was drawn from the headspace of the equilibrator and continuously pumped through the instruments and then back to the equilibration chamber forming a closed loop. The air stream was dried before being injected into the analysers by means of a Nafion® tube in order to diminish interferences due to the water vapour content of the sample. The water temperature was constantly monitored by means of a high accuracy digital thermometer placed in the equilibrator. Ambient air measurements were accomplished by pumping air into the system from a suction point located at the ship's fore mast at about 30 m height. Furthermore, control measurements and calibration procedures were performed every 24 h using two standard gas mixtures and compressed air, thereby bracketing the expected N_2O, CO and CO_2 concentrations.

Discrete comparison samples for N_2O and CO_2 were taken regularly by sampling from the same water stream that fed the underway setup. N_2O samples were measured on board as described above, whereas samples for dissolved inorganic carbon (DIC) and total alkalinity (TA) were collected and stored to be measured at the Chemical Oceanography department of the GEOMAR in Kiel. In order to better understand the biogeochemical processes affecting dissolved gases in the surface ocean, samples for nutrients, chlorophyll a and coloured dissolved organic matter (CDOM) were taken from the continuous seawater supply. Measurements of nutrients (nitrate, nitrite, phosphate and silicate) were performed on board by using a QuAAtro (Seal Analytical, Norderstedt, Germany) segmented flow analyser in cooperation with Kerstin Nachtigall (see section on nutrient analysis for detailed information), chlorophyll a samples were filtered and analysed on board by using a fluorometer in cooperation with Violeta Leon, IMARPE (see section on chlorophyll sampling for detailed information). Filtered samples of seawater from the underway setup were also analysed for CDOM in cooperation with Luisa Galgani and Jon Roa (see section on surface microlayer sampling for detailed information). In total, 31 samplings from the underway system for N_2O, DIC/TA, nutrients chlorophyll a and CDOM were performed during the cruise.

5.11.3 Discrete N_2O and CH_4 sampling

5.11.3.1 N_2O

N_2O profiles were taken at 43 stations from the CTD rosette. Triplicate samples were taken in 20 mL opaque glass vials without bubbles and sealed with butyl rubber stoppers and aluminium caps. A 10 mL helium headspace was added directly after the sampling with a gas tight syringe. Samples were subsequently treated with 50 µL of a mercuric chloride solution (0.07 mol L^{-1}), shaken vigorously and left to equilibrate for a minimum of 2 h. A 9-9.5 mL subsample was drawn from the equilibrated samples and manually injected into a GC-ECD system (HP 5890 II). For details of the analytical method see Kock et al. (2012).

5.11.3.2 CH_4

CH_4 samples were taken from 9 stations of the Callao Time Series Transect (Transect F). Triplicate samples were taken in 50 mL glass vials without bubbles and sealed with butyl rubber stoppers and aluminium caps. The samples were treated with 50 µL of a saturated mercuric chloride solution to avoid biological production or consumption of CH_4. The caps were sealed with paraffin wax and the samples were transported to Kiel by air freight in upside down position. GC analysis of the samples will be done at GEOMAR.

5.11.3.3 Zodiac Sampling

In the upper 1 m, samples were taken using a custom-made submersible pump that continuously pumped water from an adjustable depth into the zodiac. Six samples per depth were taken from four to five depths. Samples from five to six depths between 1 and 10 m were taken using a 3.5 L Niskin bottle (HydroBios, Kiel, Germany) that was released on a rope by hand.

Except for the last profile, all samples were analysed on board as described above. Samples from station #1777 were treated with 50 µL of a mercuric chloride solution (0.07 mol L^{-1}). The

caps were sealed with paraffin wax and the samples were shipped to Kiel in upside down position to prevent air intrusions during the transport.

5.11.3.4 Measurement of NH_2OH, N_2H_4

Hydroxylamine (NH_2OH) and hydrazine (N_2H_4) are short-lived intermediate products in different microbial processes in the nitrogen cycle. NH_2OH is produced in the first reaction step of nitrification and during dissimilatory nitrate reduction to ammonium (DNRA), while N_2H_4 evolves as characteristic intermediate in the anammox process. Detecting these substances in the water column can help tracking down key processes in the nitrogen cycle. NH_2OH depth profiles have been published from a few marine environments. However, these measurements may be biased by the presence of nitrite which has recently been shown to interfere with the NH_2OH detection by conversion with ferric ammonium sulphate (Kock and Bange, 2013). The data obtained during M91 are among the first oceanic measurements of NH_2OH which bypass the potential bias from NO_2^-. So far, no data are available on the detection of hydrazine in seawater. Meyer (2009) developed a method for hydrazine analysis in seawater based on the oxidation to N_2O by nitrous acid. However, as the addition of nitrous acid to the samples produces significant amounts of N_2O (Kock and Bange, 2013), this background production of N_2O needs to be subtracted from the measurements, and a specific scavenger for N_2H_4 is needed. Based on laboratory experiments with different reagents, Mn^{2+} was used as a scavenger for N_2H_4 during M91.

5.11.3.5 Hydroxylamine (NH_2OH)

Hydroxylamine samples were taken at nine stations during M91. In addition to the N_2O profile, triplicate samples were taken from the Niskin bottles from selected depths. At stations 1725, 1727, 1730, 1731 and 1755, a 10 mL helium headspace was added to the samples directly after sampling and the samples were subsequently treated with 100 µL of a solution of sulphanilamide (0.01 mmol L^{-1}) in acetic acid (glacial) and 100 µL of a ferric ammonium sulphate solution (0.25 mmol L^{-1}) to convert hydroxylamine to N_2O. A standard addition series with four different hydroxylamine concentrations was conducted from one or two depths (oxygen minimum and/or surface water) per station in addition to the sampling of the depth profile for the determination of the conversion efficiency. The hydroxylamine samples were analysed for N_2O a maximum three days after sampling as described above. At stations 1736, 1759, 1762 and 1770, the samples were directly treated with 200 µL of a solution of sulphanilamide/acetic acid and 200 µL FAS solution. 10 mL of helium was added to the samples a minimum 2 h before the analysis of the samples as N_2O with the GC/ECD system described above.

5.11.3.6 Hydrazine (N_2H_4)

N_2H_4 analysis was tested at one station during M91. Two sets of triplicate samples were taken from eight depths of station 1737. The samples for background production were treated with 100µL manganese chloride solution (0.01 mmol L^{-1}). All samples were incubated for 24h at 8°C before conversion to N_2O. After 24h all samples were treated with 200 µL hydrochloric acid (2 mol L^{-1}) and 50 µL sodium nitrite (1.8 mmol L^{-1}). To determine the efficiency of the reaction between N_2H_4 and nitrous acid, 12 samples were taken in addition to the depth profile from

300 m for a standard addition of 4 different hydrazine concentrations between 0 and 100 nmol L^{-1}, which were then treated the same way. All samples were analysed for N_2O using static equilibration as described above another 24 h after the addition of nitrite.

5.11.3.7 Preliminary Results

The surface distributions of dissolved CO_2 and N_2O (both expressed as dry mole fraction in the equilibrator headspace) are shown in Figure 5.11. Measurements were performed with a novel combined analyser system (see above) which was set up at GEOMAR, allowing combined measurements of dissolved and atmospheric partial pressures of N_2O and CO_2 with unprecedented high sampling frequency and precision. With this continuously operated underway system even small scale variabilities of N_2O and CO_2 in the surfaces waters off Peru could be detected. We measured extremely high N_2O and CO_2. In the case for N_2O these are the highest surface concentrations ever measured in the surface ocean. In general, the partial pressures of both N_2O and CO_2 are associated with sites of high chlorophyll in the upwelling along the coast. However, the maxima of N_2O and CO_2 do not appear concurrent at the same coastal upwelling sites indicating that other local effect may also be important.

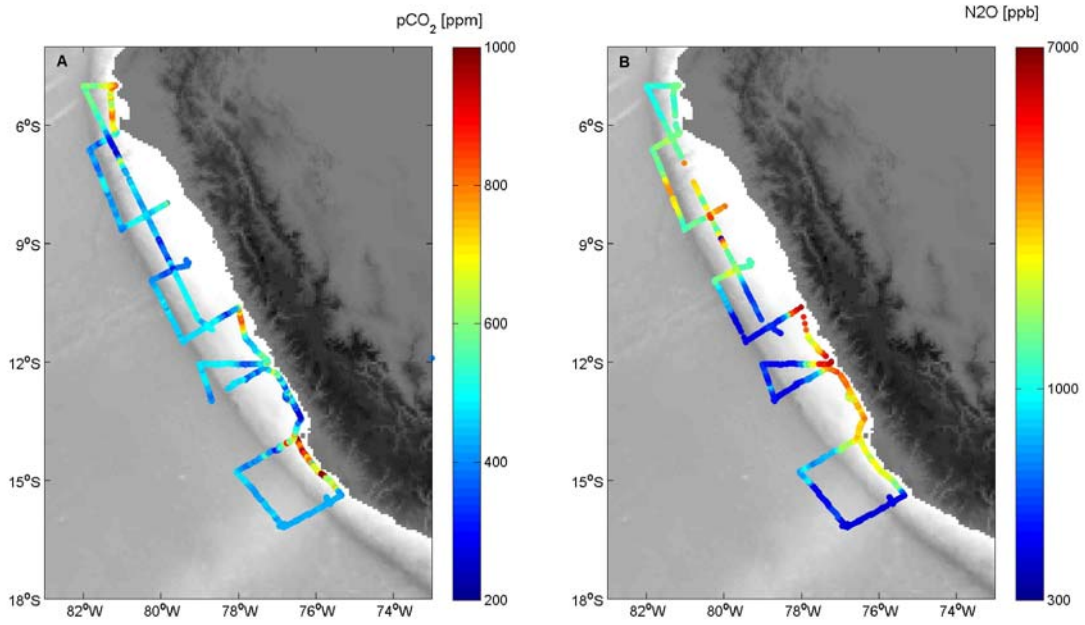

Fig. 5.11 Dissolved CO_2 and N_2O in the ocean surface layer during M91.

5.11.3.8 Time Line

We expect that the remaining samples will be analysed within a year.

5.12 Microbial Processes of the N Cycle

(Natascha Martogli, Ruth Schmitz-Streit, Carolin Löscher)

5.12.1 Dinitrogen fixation along vertical oxygen and nutrient gradients

Nitrogen is one of the key components of life and therefore a limiting element for biological primary production (Cabello et al., 2004). Atmospheric nitrogen can be made available to the ocean in form of dinitrogen (N_2) via nitrogen-fixation which is carried out by prokaryotic organisms known as diazotrophs. This process plays a key role for maintaining biological productivity in the oceans (Deutsch et al., 2007; Capone, 2008) and represents the input mechanism to the marine nitrogen cycle. In order to investigate nitrogen fixation depth profiles were sampled for analysis of the community structure of N_2-fixing microorganisms (diazotrophs) and their activity and thus the overall input of new nitrogen into the ecosystem. To examine the direct (O_2) and indirect (N/P) effects of O_2 on rates of N_2-fixation and the functional gene diversity of diazotrophs, 4.5 L samples were taken from the CTD rosette (5 to 9 different depths), fertilized with labelled N_2 ($^{15}N_2$) and incubated for 24 h in either on deck incubators which were continuously filled with ocean surface water and simulated a light attenuation at 15 m water depth or in the cold room with the approximately in situ temperatures using the method developed by Mohr et al. (2010). In order to compare dinitrogen fixation to primary production also ^{13}C bicarbonate was added to the samples alongside the $^{15}N_2$. At the end of each experiment samples for several parameters were taken including DNA/RNA, flow cytometry and label uptake (^{13}C bicarbonate and $^{15}N_2$). A total of 15 experiments were performed with a total of 85 samples. The samples for dinitrogen fixation were dried at 42 °C for 4 h and stored at room-temperature until analysis in the lab of Ruth Schmitz-Streit using mass spectrometry.

5.12.2 Nitrous oxide (N_2O) Production along Vertical Profiles

The oxygen concentrations in the eastern tropical South Pacific (ETSP) are among the lowest concentrations measured in the oceans reaching oxygen concentrations well below 20 µmol L^{-1} (Fuenzalida et al., 2009). This very shallow oxygen minimum is closely coupled to the coastal upwelling along the Peruvian coast enabling the emission of large amounts of greenhouse gases such as nitrous oxide (N_2O) and carbon dioxide (CO_2) to the atmosphere (Paulmier et al., 2008). Nitrous oxide can be produced both during denitrification and nitrification, but only during the latter it is able to accumulate in the water column and therefore reach the atmosphere. Nevertheless, there is only sparse information available about in situ production of the greenhouse gas N_2O via nitrification, therefore the biological production of nitrous oxide and the thus resulting flux of this potent greenhouse gas from the ocean to the atmosphere was investigated by conducting incubation experiments in either on deck incubators or in the cold room at approximately in situ temperatures.

Small water samples were taken at two to eight different depths at a total of 14 stations (127 samples) and incubated for 24 h. Alongside, incubations with the addition of the archaeal inhibitor N1-guanyl-1.7-diaminoheptane (GC7) or the bacterial inhibitor Dicyandiamid (DCD) were conducted to gain an insight into the producing organisms, some samples were also fertilized with 10 µmol L^{-1} ammonia. All samples were taken as triplicates in 50 ml glass vials, closed airtight and conserved with mercury chloride ($HgCl_2$) after the incubations.

Measurements and evaluations of N_2O samples will take place in the labs of Hermann Bange and Ruth Schmitz-Streit.

5.12.3 Hydroxylamine (NH_2OH) Production along Vertical Profiles

Hydroxylamine is formed during one of the major microbial processes of the marine nitrogen cycle: nitrification (Arp and Stein, 2003), assuming it to be the main production pathway (Gebhardt et al., 2004; Santoro et al., 2011). Both Bacteria and Archaea are nitrifying microorganisms producing N_2O as a by-product (Santoro et al., 2011; Löscher et al., 2012), but until now hydroxylamine as an intermediate product and a precursor of N_2O has only been identified for bacterial nitrification.

So far, in marine environments only nanomolar to submicromolar concentrations of hydroxylamine are traceable during its production and consumption by nitrifying microorganisms (Butler and Gordon, 1986). Therefore the investigation of the in situ hydroxylamine production during the coastal upwelling along the Peruvian coast could deliver a better insight into the production pathway itself and the effects of different influences and stress factors, i.e. nutrient input, oxygen minimum, inhibitors and fertilization.

Hence alongside the nitrous oxide incubations also incubations for hydroxylamine were conducted at 7 stations (52 samples) using either on deck incubators or the cold room with approximately in situ temperatures. Alongside also incubations using different inhibitors (GC_7 or DCD) or ammonia as a fertilizer were conducted. All samples were taken as triplicates in 50 ml glass vials, closed airtight and incubated for 24 hours. After the incubations the hydroxylamine was converted into nitrous oxide using the modified method developed by Kock (2012). Measurements and evaluations of these samples will take place in the labs of Hermann Bange and Ruth Schmitz-Streit.

5.12.4 DNA/RNA Sampling and Flow Cytometry

Samples for DNA/RNA were taken at ~12 depths with a total of 25 sampled stations. Small volume (2 L) DNA/RNA samples were filtered through 0.2 µm membrane filters (Millipore, Isopore membrane filters) within a time frame of 20 min directly after collection from the CTD rosette to prevent temperature and light responses in the RNA. Filters were immediately frozen and stored at -80 °C. Alongside 980 µL of these samples were fixed with 20 µL formaldehyde (37 %) and stored at -20 °C for later analysis in the flow meter.

DNA and flow cytometry samples were taken back to the home laboratory in frozen condition for further analysis. In total 338 DNA and 338 flow cytometry samples were taken.

DNA/RNA samples will be analysed regarding microbial diversity and gene activity in the lab of Ruth Schmitz-Streit. The microbial gene diversity will be analysed focusing especially on the genes involved in the marine nitrogen cycle. A newly developed microarray will be used to screen for N cycle genes, results will be verified by quantitative Real Time PCR, sequencing and deep sequencing. To determine the extent to which phylogenetically-related diazotroph ecotypes as well as other microorganisms involved in the nitrogen cycle are adapted to specific nutrient stoichiometry and O_2 concentrations a metagenomic and metatranscriptomic approach will be used. Also the phylogenetic diversity of 16S rDNA, the *nifH* and the *amoA* genes will be monitored.

5.13 Nitrogen Isotopes and N_2/Ar

(Annie Bourbonnais, Chawalit Charoenpong, Mark Altabet)

5.13.1 Scientific background and study goals

Nitrogen (N) is an essential and often limiting macronutrient for primary producers in the surface ocean. As a consequence, it is an important modulator of the marine biological pump and of the ocean's capacity to sequester atmospheric CO_2, a greenhouse gas, in its interior (Falkowski, 1997). The availability of bio-available N in marine environments is regulated by the balance between N sources, mainly from N_2 fixation, and N loss by denitrification and anaerobic ammonium oxidation (anammox), both of which occur under hypoxic conditions ($[O_2] < 10$ μmol L^{-1}) and convert dissolved inorganic N to gaseous N_2. It is an on-going debate whether the marine N budget is in or out of balance, as large errors are associated with current estimates (Codispoti, 2007). Additionally, N_2O, a potent greenhouse gas, is produced and/or consumed during denitrification and nitrification in oxic waters. An on-going expansion of oxygen minimum zones (OMZs) in the ocean has been observed over the last decades (Stramma et al., 2008), with potential important implications on global climate. OMZs are located in well-constrained ocean regions with high surface primary productivity and low oxygen source waters. Although they represent only 0.1 % of total oceanic volume, OMZ's host the largest portion of total marine N loss (up to 400 Tg yr^{-1}; Codispoti, 2007) and dominate the ocean N isotope budget through co-generation of ^{15}N and ^{18}O enriched NO_3^- (Cline and Kaplan 1975; Voss et al., 2001; Sigman et al. 2005) and ^{15}N depleted N_2. A better understanding of N-loss rates in OMZ's and their controls is primordial to better assess the ocean's capacity to fix carbon dioxide under current and future conditions.

Stable isotope measurements represent a useful tool to study N cycle transformations in marine environments. Both NO_3^- assimilation and denitrification increase the NO_3^- $\delta^{15}N$ (with $\delta = [(R_{sample}/R_{standard})-1] \times 1000$, where R represents the ratio of ^{15}N to ^{14}N) as a consequence of kinetic N-isotope fractionation (e.g. Cline and Kaplan (1975) and reference therein). An N isotope enrichment factor ($\varepsilon_{ass} \approx \delta^{15}N_{substrate} - \delta^{15}N_{product}$) of ~5‰ has been reported for NO_3^- assimilation (Altabet, 2001). The isotope enrichment factor (ε_{den}) associated with microbial denitrification is high, with most recent estimates from both laboratory experiments and natural environments clustering between 20 and 25 ‰ (Brandes et al., 1998; Voss et al., 2001; Granger et al., 2008). While N isotopes alone can provide qualitative and semi-quantitative information on single N cycle transformations, they are less informative in oceanic regions where several N-transformations have overprinting effects on both the NO_3^- concentration and N isotope signatures. However, the measurement of coupled NO_3^- N and O isotope ratios has the potential to disentangle NO_3^- consumption and production processes in environments where they occur simultaneously (Sigman et al., 2005; Casciotti and McIlvin, 2007; Bourbonnais et al., 2009; 2012). This is possible because the $\delta^{15}N$ and $\delta^{18}O$ of NO_3^- are affected in fundamentally different ways during NO_3^- consumption and production (e.g. see Sigman et al., 2005; Bourbonnais et al., 2009; 2012).

The unusual inverse fractionation effect for NO_2^- oxidation (Casciotti et al. 2009, $\varepsilon \sim$ -14 to -20‰) represents a potentially powerful approach to help distinguish processes controlling both the NO_3^- $\delta^{18}O$:$\delta^{15}N$ relationship and the production of biogenic N_2. For denitrification, $\delta^{15}NO_2^-$ would be a function of the difference in ε values for NO_3^- and NO_2^- reduction. Since they are

similar in magnitude (Bryan et al., 1983), $\delta^{15}NO_2^-$ should be similar to $\delta^{15}NO_3^-$. However if NO_2^- oxidation is a significant fraction of these fluxes, $\delta^{15}NO_2^-$ is lower, as observed in the eastern tropical North Pacific Ocean consistent with either extensive cycling between NO_3^- and NO_2^- and/or important fluxes to NO_3^- via oxidation of low $\delta^{15}N$ NH_4^+.

The large isotopic and isotopomer signatures associated with N_2O production and consumption yield important source/sink information (Yoshinari et al., 1997; McIlvin and Casciotti, 2010). In addition to bulk $\delta^{15}N$ and $\delta^{18}O$, the asymmetry of the N_2O molecule permits distinguishing the N isotopic composition of the central (a) and end (b) position N atom (^{15}N site preference (SP) is defined as $\delta^{15}N^{\alpha}$ - $\delta^{15}N^{\beta}$) (Yoshida and Toyoda, 2000), which is distinct for N_2O resulting from nitrification or denitrification, and thus potentially allow to differentiate between these different processes.

Our main goals during the research cruise M91 was to collect samples along hydrographic sections for analysis of:

a) Dissolved inorganic N (DIN) isotopes: NO_3^- and NO_2^- $\delta^{15}N$ and $\delta^{18}O$, NH_4^+ $\delta^{15}N$ and dissolved organic N (DON) $\delta^{15}N$.
b) N_2/Ar and $\delta^{15}N_2$.
c) N_2O $\delta^{15}N$ and $\delta^{18}O$ and ^{15}N site preference (in collaboration with Hermann Bange).
d) Near-surface POM $\delta^{15}N$.

5.13.2 Methods

5.13.2.1 DIN isotope analysis

NO_3^- is analysed by Cd reduction to NO_2^- followed by reaction with azide (HN_3) to produce N_2O in sealed septum vials (McIlvin and Altabet 2005) with modifications to prevent over-reduction. When sulphamic acid has been added to remove NO_2^-, no interference occurs from leftover reagent due to maintenance of a high pH until addition of the azide reagent as sulphamic acid reacts with NO_2^- (actually HNO_2) only at low pH. N_2O gas is analysed using a purge-trap interface (Sigman et al., 2001) to a GV IsoPrime IRMS. Reproducibility is ± 0.2 ‰ for $\delta^{15}N$ and ± 0.4 ‰ for $\delta^{18}O$ on sample concentrations as low as 0.5 µmol kg^{-1}. Standardization is against publicly available and certified materials (e.g. USGS32, USGS34, and USGS 35).

NO_2^- isotopic composition is measured without prior Cd reduction using a modification of the azide method. These samples are preserved frozen at pH 12 and buffering of the azide reagent is adjusted to bring the pH down to the reaction favourable range of 4 to 5 without O isotope exchange with water. Publically available standards are not yet available but we have exchanged materials with Karen Casciotti's lab.

Where $[NH_4^+]$ > 0.5 µmol kg^{-1}, its $\delta^{15}N$ is measured by hypobromide oxidation to NO_2^- followed by the azide reaction to N_2O (Zhang et al., 2007). Prior removal of NO_2^- by sulphamic acid is equally effective in this case. DON $\delta^{15}N$ can be measured using persulphate oxidation to NO_3^- (Knapp et al. 2005) though these latter analyses will be pursued only on an ancillary, exploratory basis.

5.13.2.2 Dissolved gases analysis

N_2/Ar and $\delta^{15}N_2$ analyses are made by pumping, at 5 to 10 ml min^{-1}, water samples through a continuous sparger which transfers dissolved gases quantitatively to a continuous flow of He carrier gas. Dissolved gas samples require no preparation in the lab and analysis time is about 10 min. Carrier gas is passed through water, CO_2, and software selectable hot-Cu O_2 traps before admittance via an open split to an IRMS. O_2 removal improves the precision of the N_2/Ar and $\delta^{15}N_2$ measurements and eliminates analytical bias associated with changing sample O_2/N_2. Our GV IsoPrime IRMS is fitted with sufficient collectors for simultaneous measurement of N_2 (masses 28 and 29), O_2 (masses 32, 33, and 34), and Ar (mass 40). Gas and isotopic ratios are measured against artificial compressed gas mixtures of N_2, O_2, and Ar close to expected dissolved gas ratios. These reference mixtures are in turn calibrated against compressed air cylinders provided and certified by Ralf Keeling (SIO). Reproducibility of N_2/Ar and $\delta^{15}N_2$ is better than 0.5 ‰ and 0.05 ‰, respectively. Daily calibration is against water equilibrated with air at precisely controlled temperatures of 10.0 and 20.0 °C. Excess (biogenic) N_2 will be initially calculated against equilibrium values expected from in situ temperature and salinity.

5.13.2.3 N_2O isotopomer analysis

This work will be in collaboration with Hermann Bange. Analyses will be made directly on samples using a PT-IRMS system, as described above, except for additional time needed for sample gas extraction from the larger volume. Back flushing of the purge-trap system's GC column as recommended by McIlvin and Casciotti (2010) has already been implemented to eliminate interferences in the ^{15}N site preference (SP) determination. Our IRMS has the necessary collector configuration for simultaneous determination of masses 30, 31 (for SP) and 44, 45, and 46 (bulk $\delta^{15}N$ and $\delta^{18}O$). A multiple point calibration of several N_2O gases of known SP (as well as bulk $\delta^{15}N$ and $\delta^{18}O$) will be applied. We plan to exchange reference gases with Karen Casciotti's lab as a first approach to calibration with subsequent curve fitting and solving for the appropriate parameters.

5.13.2.4 POM $\delta^{15}N$ analysis

POM $\delta^{15}N$ is measured using an elemental analyser coupled to the IRMS.

5.13.3 Time line

Early in Year 1 of the U Mass. project (late 2012/early 2013), the three R/V Meteor cruises (M90, M91 and M92) will take place constituting the field program for this project. Dissolved gas (N_2/Ar) sample analysis will immediately commence for completion within 6 months of collection. In Year 2, DIN and N_2O sample analysis will be the primary activity. We anticipate concluding analytical activity at the end of the second year and start initial data workup and interpretation. N_2O samples have a much longer longevity as compared to dissolved gas samples and their analysis can occur this long after collection. In Year 3, results will be written up for publication.

5.14 Sea-Surface Microlayer

(Luisa Galgani, Jon Roa, Anja Engel)

5.14.1 Scientific Background

The sea-surface microlayer (SML) is a specific ecosystem at the water-air interface resulting from the accumulation of organic matter released by microbial metabolic activity at the surface. It has been shown that the SML is a boundary layer with a gel-like nature (Cunliff and Murrell, 2009) which can be described as a gelatinous matrix of varying thickness entrapping several compounds like lipids, carbohydrates, proteins and specific bacterial communities known as bacterioneuston (Sieburth, 1983; Liss and Duce, 1997). In the SML carbohydrates and proteins are also present as marine gels like Transparent Exopolymer Particles (TEP) of polysaccharidic composition and Coomassie-stainable Particles (CSP) of proteinaceous composition. These compounds are released by the metabolism of phytoplankton and bacteria promote microbial biofilm formation and mediate vertical carbon transport, either to the sea-surface or to the deep ocean. The presence of surface films can lead to the formation of visible slicks that lower seawater tension thus affecting gas-exchange between the ocean and the atmosphere.

For this reason, we drove our attention to organic matter components and turnover at the surface because the gelatinous character of SML represents a key-issue for gas fluxes. Microbial activities in the SML, like the release of biological exudates, continuously alter its composition and render the very surface of the sea a unique and mutable environment. In particular, heterotrophic bacteria have been shown to respond to rising CO_2 and sea-surface temperatures (Piontek et al., 2010) and their activity in the SML is crucial to understand future feedbacks of global warming. In the coastal upwelling region off Peru enhanced emission of oceanic trace gases may strongly affect climate and atmospheric dynamics. In this respect, investigating the composition of the boundary layer at the water-air interface becomes of great importance for our understanding of the exchange processes relevant for climate change.

5.14.2 Parameters measured

During the M91 cruise we have focused on sea-surface microlayer composition in terms of DOM dynamics in the surface ocean. For comparison, samples from 20 cm below the surface and CTD casts were taken. 41 stations were sampled for sea-surface microlayer from a zodiac. This sampling procedure could be made only during daylight hours. According to zodiac deployments, in 21 stations six depths from the CTD cast have been sampled. The depths were chosen depending on chlorophyll and oxygen profiles, and in particular:

- Depth 1 – surface depth
- Depth 2 – chlorophyll maximum
- Depth 3 – beginning of OMZ
- Depth 4 – minimum oxygen
- Depth 5 – one depth below minimum oxygen
- Depth 6 – deep depth for oldest and more refractory dissolved organic matter (DOM).

Our measurements include dissolved and total organic carbon (DOC and TOC), total nitrogen and total dissolved nitrogen (TN and TDN), chromophoric dissolved organic matter and

fluorescent dissolved organic matter (CDOM and FDOM), total and dissolved combined carbohydrates, total and dissolved hydrolysable amino acids, bacterial cells number and phytoplankton cells number, and marine gels like TEP and CSP. CDOM and FDOM have been measured directly on board while all other parameters have been stored cooled or frozen for further processing in our laboratory at GEOMAR in Kiel.

5.14.3 Methods

The sea-surface microlayer has been sampled with the glass plate approach: a glass plate of 20 x 50 cm has been introduced slowly into the water surface, then withdrawn and the film stacked on both sides of the plates has been removed with a Teflon wiper. Samples for DOC (and TDN) have been filtered through pre-combusted (8 hours, 500 °C) GF/F filters into pre-combusted and sealed ampoules and stored cooled. TOC/TN samples have received the same treatment except for filtration, and analysis for both will be performed in a Shimadzu TOC – VCSH analyser with Total Nitrogen (TNM-1) unit. CDOM and FDOM samples have been filtered through 0.45 µm single use filters. CDOM absorbance has been measured in a Shimadzu UV-1800 UV-Spectrophotometer in the range 200-700 nm with 0.5 nm increments. FDOM has been measured in a Cary Eclipse Fluorescence Spectrophotometer in order to get Excitation/Emission matrices which enable to individuate the single fluorophores of DOM. Scans have been performed at 600 nm min^{-1} with excitation in the range 200-450 nm with 5 nm increments, recording emission in the range 220-600 nm (Stedmon et al., 2008; Coble, 1996). Samples for carbohydrates and amino acids have been stored in pre-combusted vials and stored frozen at -20 °C, and those for the dissolved fraction have been additionally filtered through 0.45 µm. Analysis for carbohydrates will be performed with Ion Chromatography following the protocol by Engel and Händel (2011) while amino-acids samples will be analysed with HPLC. Samples for bacterial cell numbers and phytoplankton cell numbers have been preserved with GDA 25% and stored frozen. Cells will be enumerated in Kiel by flow-cytometry in the next three months. TEP and CSP are determined filtering the samples through polycarbonate membranes of 0.4 µm pore size, then the membranes are stained for TEP with Alcian Blue solution or Coomassie Brilliant Blue solution for CSP. For microscopy analysis, filters are stored frozen on microscope slides. Additionally to the microscopy analysis, TEP concentration will be determined with the colorimetric method (Engel, 2009).

5.14.4 Time Line

We expect that in the time frame of one year, all samples will be analysed and data available.

5.15 Air-Sea Gas Exchange, Wind Waves, CO_2 Eddy Covariance

(Daniel Kiefhaber, Leila Nagel, Bernd Jähne, Christopher Zappa)

5.15.1 Scientific Background

The investigation of the cycles of trace gases such as CO_2 requires the determination of fluxes between atmosphere and ocean. The direct measurement of these fluxes is difficult and possible only for a few species. However, if the transfer velocity for gas exchange is known, fluxes can be computed from measured concentration differences between air and water. Since heat and

gases are transported by the same physical processes, gas transfer velocities can be calculated based on measured heat transfer velocities.

Transfer velocities (for water-side controlled gases with low solubility) are controlled by near surface turbulence. Since it is nearly impossible to directly measure turbulence very close to the surface from a ship, wind speed is typically used as a parameter. However, the relationship between wind speed and turbulence and thus transfer velocities is not straightforward. Wind creates waves and a shear current; both can contribute to the turbulence level below the surface. Especially in the presence of surfactants (which are very common in areas with high biological activity), the wave field is significantly altered: the surface is much smoother as small-scale waves are effectively dampened by the surfactants. This leads to a decrease in turbulence and thus gas transfer velocity which is not included in wind speed parameterizations. By measuring the sea state directly, this problem can be avoided and wave field characteristics (e.g. the mean square slope, a measure for surface roughness) can be used directly as parameters for the transfer velocity.

5.15.2 Measurements

Our instrumentation that was set up at the bow of Meteor consisted of four instruments:

- Active Controlled Flux Technique (ACFT) Instrument: measures local transfer velocities
- Reflective Stereo Slope Gauge (RSSG): measurements of sea surface roughness (mean square slope), wave heights, wave frequency spectra at the same footprint as ACFT
- Stereo Polarimeter (SP): experimental instrument, measurements of 2D slope and height maps of the sea surface, wavenumber/frequency spectra of waves
- Eddy covariance (EC) system: turbulent fluxes of momentum (friction velocity), heat, CO_2, H_2O

The Table 5.15 below gives an overview of the stations at which the different instruments were acquiring data. The EC system was recording data continuously, but data can only be processed if the ship was heading into the wind. On the transit after station 1736-2, the system's 3D anemometer was damaged. It is unclear if data acquired past this point usable after recalibration. The SP is an experimental instrument that only works well at day and when the sky is completely overcast so it was not used most of the time.

Tab. 5.15: Overview of measurements.

Station	ACFT	RSSG	Stereo Pol	Eddy Cov
1713-1	•			•
1713-2	•			•
1715-2	•	•		•
1717-2	•	•		•
1719-2	•	•		•
1721-1	•	•		•
1721-2	•	•		•
1724-2	•	•		•
1725-2		•		•
1727-2	•	•		•
1729-2	•	•		•
1733-2	•	•		•
1733-3	•	•		•
1733-4	•	•		•
1733-7	•	•		•
1733-8	•	•		•
1733-10				•
1733-12				•
1736-2	•	•		•
1737-2	•	•		o
1739-2	•	•		o
1741-2	•	•		o
1746-2		•	•	o
1748-2	•	•		o
1749-2	•	•		o
1750-2	•	•	•	o
1751-2	•	•		o
1752-3	•	•		o
1752-6	•	•	•	o
1752-10	•	•		o
1752-11	•	•		o

Station	ACFT	RSSG	Stereo Pol	Eddy Cov
1755-3	•	•		o
1756-2		•		o
1759-2				o
1760-2		•		o
1761-3		•	•	o
1762-3	•	•		o
1763-2	•	•		o
1764-2		•	•	o
1764-5	•	•	•	o
1764-10	•	•	•	o
1764-11	•	•		o
1766-2	•	•	•	o
1768-2		•		o
1769-2		•	•	o
1770-2	•	•	•	o
1771-2	•	•		o
1772-2	•	•		o
1773-1	•	•	•	o
1773-4	•	•		o
1774-2	•	•	•	o
1775-2	•	•		o
1776-2	•	•	•	o
1777-3	•	•	•	o
1777-6	•	•		o
1777-8	•	•		o
1777-9	•	•	•	o
1778-2	•	•	•	o

5.15.3 Methods

5.15.3.1 Active Controlled Flux Technique (ACFT)

The transfer velocity can be determined by measuring concentrations in air and water and the flux between atmosphere and ocean. Using heat, the flux measurements can be avoided by forcing a well-known flux density to the water surface. This is done by a CO_2-Laser. The temperature difference between heated and unheated area is determined out of thermal images, taken from the water surface. Switching on the Laser, the thermal images show an increasing temperature until a thermal equilibrium is reached. The temperature difference between the heated an unheated water surface can be detected out of a sequence, when the laser is switched on and off with low frequencies. Especially at day time, reflections of the sun or the warm ship can overlap the data and must be corrected.

5.15.3.2 Wave Measurements

Both wave measuring instruments, the RSSG and the SP, use light reflected at the water surface to obtain information on the wave field. The RSSG has built-in light sources and filters to block out skylight, so it can measure under most conditions, day and night. It uses stereo triangulation to measure wave heights and a statistical method to measure surface roughness. The SP can measure the shape of the two-dimensional wave field by stereo triangulation and by measuring

the polarization of the skylight that is reflected at the water surface. It is a passive instrument that works best with a completely overcast sky.

5.15.3.3 Direct Flux Measurements

By measuring the correlations between fluctuations of trace gas concentrations (or temperature) and fluctuations of wind speed (eddy covariance), it is possible to directly quantify air-sea fluxes. The eddy covariance package measures fluxes of CO_2 and H_2O, as well as heat and momentum fluxes. Instrumentation includes an ultra-sonic anemometer that measures 3D wind speed and temperature, an open path CO_2/H_2O gas analyser as well as instruments measuring radiation, relative humidity and ship motion.

5.15.4 Time Line

The acquired data requires complex post-processing. Especially for the imaging techniques this includes significant computational time. The final results are expected to be available in autumn 2013.

5.16 Volatile Organic Compounds (VOCs) and Oxygenated Volatile Organic Compounds (OVOCs)

(Patrick Veres, Wei Song, Bettina Derstroff, Jonathan Williams)

5.16.1 Introduction

Atmospheric volatile organic compounds (VOCs) play an important role in the production of environmental pollutants via involvement in photochemical processes (Class and Ballschmitter, 1988). VOCs and oxygenated organic compounds (OVOCs) play key roles in the production of ozone, photooxidant cycling (Lewis et al., 2005) and the formation of secondary organic aerosol (Gannt et al. 2009; Luo and Yu, 2010), which in turn influence air quality and climactic forcing. The oceans play a substantial role in global atmospheric budgets for VOCs and OVOCs serving both as a source and sink (Fischer et al., 2012; Broadgate et al., 1997; Gist and Lewis, 2006). Many of these atmospheric trace gases are produced as a result of biological activity or photochemical activity at the surface interface; however, many of the factors which control partitioning remain unknown or poorly understood. Through simultaneous measurement of gaseous and dissolved organics in parallel to the diverse measurements of biological activity and oceanic flux rates aboard the Meteor cruise M91 we hope to better understand the factors that control the magnitude and direction of VOC fluxes in the lower marine atmosphere.

5.16.2 Instrumentation

High time resolution measurements of ambient mixing ratios of VOCs were performed using a commercial proton-transfer-reaction time-of-flight mass spectrometer (PTR-TOF-MS) from Ionicon Analytik GmbH (Innsbruck, Austria). Mass spectra were collected ranging from m/z 10 - 350. Continuous mass spectra were collected and averaged such that the time resolution of the measurements was set to 30 seconds. Post-acquisition data analysis will be performed according to procedures described elsewhere (Mueller et al., 2011; Mueller et al.; Titzmann et al., 2012).

VOC concentrations are reported in parts-per-billion by volume (ppbv) when calibration data is available; otherwise normalized counts per second (ncps) are reported. Measurements of ozone were performed using a commercial UV photometric ozone analyser (Thermo Environmental). The ozone analyser was operated at a time resolution of 10 seconds throughout the duration of the experiment. Dissolved VOCs measurements were performed during the M91 cruise using needle Trap device gas chromatograph mass spectrometry (NTD-GC-MS), a novel analytical method recently developed. The technique uses needle trap devices (PAS technology) and a gas chromatograph (Agilent 6890) coupled to an electron impact mass spectrometer (Agilent 5973 inert) operated in selected ion mode. The commercial NTDs consist of a 23-gauge, 60 mm long stainless steel needle packed with 10 mm each of polydimethyl siloxane (PDMS), Carbopack X and Carbon 1000. A ß-cyclodextrin capillary column (Cyclodex-B, 30 m long, 250 µm ID, 0.25 µm film thickness) (J&W) was used to resolve selected VOCs.

5.16.3 Measurements

The PTR-TOF-MS instrument was installed in the atmospheric chemistry laboratory on the uppermost deck of the Meteor. A 30 m unheated 1/2" Teflon inlet line was installed from the top of the ship's mast leading into the atmospheric chemistry laboratory supplying a continuous flow of air (~ 30 L min^{-1}) to the laboratory. The PTR-TOF-MS subsampled this flow at 100 cm^3 min^{-1} through a 1/16" PEEK inlet line heated to 60 °C. A collocated ozone analyser sampled at a flow of approximately 17 L min^{-1} through a second 5 m unheated 1/4 " Teflon inlet line installed on the roof of the atmospheric chemistry laboratory. Atmospheric VOC measurements in parts-per-billion by volume (ppbv) will be reported on a 1 minute timescale for two periods, 04/12/12 21:30:00 UTC to 07/12/2012 15:00:00 and from 10/12/12 00:00:00 until 23/12/12 23:59. Table 5.16 contains a partial list of compounds for which final data in ppbv will be readily available. For the needle trap GC-MS technique, a 10 ml Sea water sample was transferred through a glass filter (0.7 µm mesh, 25 mm, Whatman GF/F) into a purging glass tube. Seawater samples were heated and kept at 35 °C while purged with helium at a flow rate of 30 ml min^{-1} for 5 min.

Tab. 5.16. Observed mass (m/z), elemental composition (EC) and identity of atmospheric VOCs and OVOCs observed during the M91 cruise.

m/z	EC	Identity	Detection limit (3σ, pptv)
33.0335	CH_4O	Methanol	300
42.0338	C_2H_3N	Acetonitrile	70
45.0335	$C_2H_4O_2$	Acetaldehyde	100
59.0491	C_3H_6O	Acetone	70
63.0263	C_2H_6S	Dimethyl sulphide	25
69.0699	C_5H_8	Isoprene	90
71.0491	C_4H_6O	Methyl ethyl ketone	40
73.0648	C_4H_8O	Methyl vinyl ketone	40
79.0542	C_6H_7	Benzene	40
93.0699	C_7H_8	Toluene	30
107.0855	C_8H_{10}	Xylene	30
121.1012	C_9H_{12}	Trichlorobenzene	30
137.1325	$C_{10}H_{16}$	Terpenes	70

Dissolved VOCs are efficiently extracted from the sea water and trapped onto the sorbents in the needle. The NTD is subsequently sealed and inserted into GC injector for 30 s. The GC column temperature was kept initially at 40 °C for 5 min and then increased to 70 °C, at 1.5 °C min^{-1}. Helium is used as carrier gas at a flow rate of 0.8 ml min^{-1}. Measurements are calibrated using a custom chemical standard containing 19 VOCs (Sigma Aldrich, Germany) in water diluted to around 100 ng L^{-1}. Sea water samples were taken from 34 stations with different depths (5 to 9 depths from the first 100 m and 2-3 from 100 - 2000 m). 32 underway water samples and 3 zodiac samples (5 or 6 depths for each) were taken for the whole cruise.

5.16.4 Preliminary Results

Figure 5.16 shows a summary of DMS measurements made aboard the M91 cruise between 04/12 – 22/12. The ship track is coloured by observed atmospheric DMS concentrations. DMS mixing ratios ranged from below the detection limit (~ 25 pptv) up to 7 ppbv. Inset in Figure 5.16 are two 24-hour periods during stationary measurement sites the location of which are indicated by black circles. These stations allow for observation of the diurnal behaviour of VOCs on 24-hour timescales. The upper inset figure shows a behaviour typical of what was observed during the M91 cruise where DMS concentrations increase throughout the night under a low boundary layer and are significantly reduced throughout the day. In comparison, DMS measurements at the second station (lower left panel) suggest a more substantial daytime source of DMS. In conjunction with the dissolved phase organics and biological activity measurements that will be available, the causes of the differences in observed VOC sources can be thoroughly studied. This is just one brief example of how the data collected during the M91 cruise can be used to identify sources and potential sinks of VOCs in the marine atmosphere.

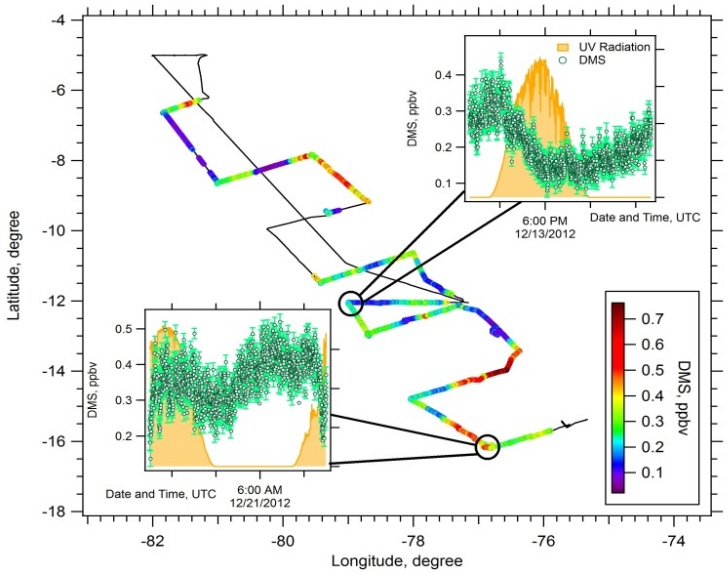

Fig. 5.16 M91 ship track for a portion of the cruise colored by atmospheric DMS measurements. The inset figure shows DMS measurements during one 24-hour station, the location of which is indicated by the large black circle**.**

5.16.5 Time Line

Final data for atmospheric VOCs (PTR-TOF-MS) will be provided within 6 months of the end date of the cruise. VOC concentrations (ppbv, when available) will be reported on a 1 minute

timescale; however, data on a 30 second timescale will be available upon request. Final ozone measurements (ppbv) will be available within one month of the end of the measurement period with a time resolution of 1 minute. Final data for the dissolved VOCs measurements (NTD-GC-MS) will be available approximately one year after the end date of the cruise.

5.17 DOAS Measurements of Reactive Trace Gases

(Johannes Lampel, Martin Horbanski, Denis Pöhler, Udo Frieß, Ulrich Platt)

5.17.1 Scientific Background

Reactive halogen species (RHS) such as bromine oxide (BrO) or iodine oxide (IO) play a major role in the chemistry of ozone in both the troposphere and the lower stratosphere and thus RHS potentially influence the ozone budget on a global scale. To estimate the overall distribution of RHS, several measurement campaigns in the Marine Boundary Layer have been conducted during the last years by the Institute of Environmental Physics of the Heidelberg University. Due to their high reactivity, which results in short lifetimes of several seconds, RHS have to be measured in-situ or with remote sensing methods such as DOAS (Differential Optical Absorption Spectroscopy). Potential sources of RHS in the atmosphere are emissions from sea salt aerosols and photolytic destruction of halocarbons or inorganic precursors released from the ocean (von Glasow, 2007). Read et al. (2008) were the first who observed background concentrations of IO and BrO in the tropical MBL. They also showed by using chemistry models that the observed IO concentrations over the western Pacific Ocean cannot be explained by emissions of halocarbons only. Therefore, a strong I_2 source had to be postulated. Ground based measurements of glyoxal by Sinreich et al. (2010) and satellite observations of glyoxal and IO by Vrekoussis et al. (2009) as well as Schönhardt et al. (2012) showed relatively high concentrations of these compounds over the Peruvian upwelling area.

5.17.2 Measured Parameters

5.17.2.1 Ozone Monitor

Ozone mixing ratio in ambient air from an inlet above the air chemistry lab, portside. Detection limit approx. 1 ppb, time resolution approx. 1 min.

5.17.2.2 CE-DOAS

In-situ mixing ratios of NO_2, IO, glyoxal and water vapour with (preliminary) detection limits under optimal conditions of approximately 100 pptv, 0.5 pptv, 50 pptv and 300 ppmv, respectively, at a time resolution of 30 min. Actual recording of spectra is done in intervals of 10 s with accordingly lower detection limits. The open-path CE-DOAS setup was installed on top of the air chemistry lab of Meteor (Figure 5.17-1) after calibration and test measurements in the Geology lab of Meteor on 02 December 2012. The CE-DOAS instrument was continuously run during the cruise with breaks for calibration measurements and maintenance only.

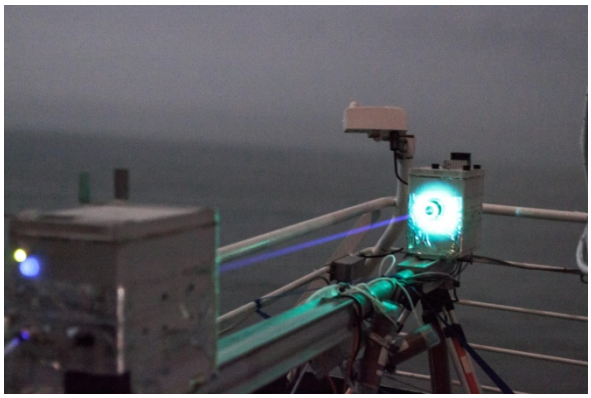

Fig. 5.17-1 Open Path CE-DOAS Setup on top of the air chemistry laboratory during a foggy night. Blue light within the resonator is clearly visible

5.17.2.3 MAX-DOAS

The used MAX-DOAS system allows the remote sensing measurements of BrO, IO, NO_2, formaldehyde, glyoxal, water vapour and ozone in the atmosphere. It can provide profile information about these trace gases in the troposphere using radiative transfer modelling methods based on the absorption of O_4. Additionally it provides overall column density information about the above mentioned trace gases in the stratosphere. The MAX-DOAS system needs sunlight for measurements. One measurement sequence for one tropospheric profile takes approximately 10 minutes. The system was set up above the bridge in the harbour of Callao on 30 November and started collected data at 20:00 UTC on that day. The measurements were stopped in the morning of 25 December 2012.

5.17.3 Methods

The ozone monitor works by measuring the ozone absorption in wave length range of UV light. The monitor is continuously switching between ambient air and ozone free air to compensate for various degradation effects. Both other methods, MAX-DOAS and CE-DOAS use the DOAS (Differential Optical Absorption Spectroscopy) principle described in Platt et al. (2008). MAX-DOAS uses scattered sunlight, which effectively travelled for several kilometres in the troposphere before it reaches the instrument. In this way it is possible to obtain long enough light paths to be able to measure at reasonably low detection limits. Modelling of the light paths is necessary to obtain actual concentrations (Frieß et al. 2006). The CE-DOAS (Platt et al. 2009) setup consists of a light source (and can therefore also measure during the night) and a detector. The light path between them is effectively multiplied by a factor of around 1000 by means of a resonator cell consisting of two highly reflective mirrors allowing in-situ measurements. The actual light path length was measured by ringdown measurements, i.e. measurements of the lifetime in the resonator of short light pulses. Additionally the light path can be measured by comparing Rayleigh scattering of dried and filtered air and helium. Depending on the aerosol load of the air and the reflectivity of the mirrors light path length of 2-6 km were measured.

5.17.4 Preliminary Results

The ozone monitor from Heidelberg and the one from Mainz showed consistent values during most of the time, though their inlets were placed 3 m apart. When sampling air from the ship's

stack, drops in ozone mixing ratios and a rise in NO_2 from the CE-DOAS data have been observed (Figure 5.17-2). External influences have been observed, e.g. by polluted air coming from land close to Trujillo several 100 km north of Lima, which led to constantly high ozone values for a couple of hours. The same feature was observed close to Lima. A preliminary evaluation of the MAX-DOAS data showed results which were comparable to those which have been measured during various campaigns in the Mauritanian upwelling and during cruises on R/V Polarstern on the Atlantic Ocean. BrO was not found in high concentrations > 5 ppt, but a rather constant background during the day of a few ppt has been observed during M91 (Figure 5.17-3). IO concentrations were found to be around 1-2 ppt, most probably slightly higher than those observed by Großmann et al. (2012) over the western Pacific Ocean. NO_2 was found downwind of towns such as Lima and Trujillo, but also in the ship plumes. Here formaldehyde was also found, but also its significant background concentrations of around 0.5 ppb were measured. Glyoxal concentrations were so far not above the detection limit of about 100 ppt, but the retrieval needs more fine-tuning as well. OIO, I_2 and SO_2 were not measured due to spectral limitations of the instrument. The preliminary data of the CE-DOAS measurements agrees well for NO_2, although they differ due to the different air masses they have measured. For IO this also seems to be the case, but obtained mixing ratios are close to the instruments' detection limit and therefore still object to optimizations.

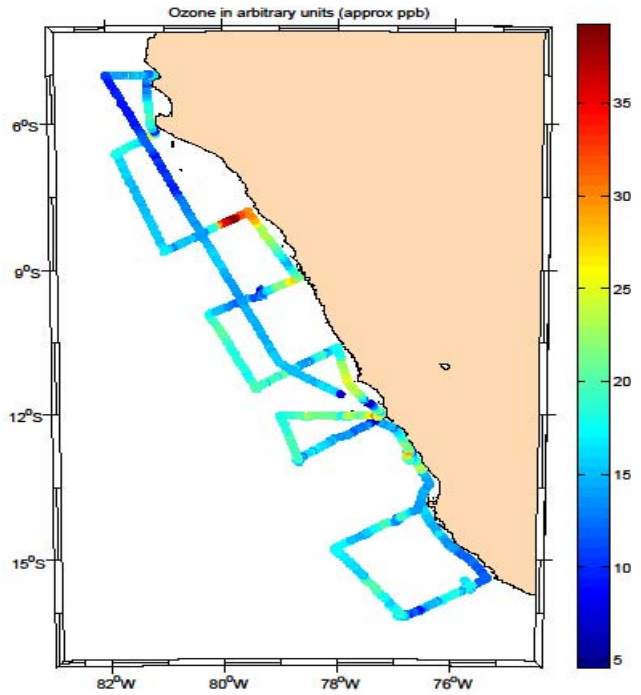

Fig. 5.17-2 Atmospheric ozone during M91.

Fig. 2:

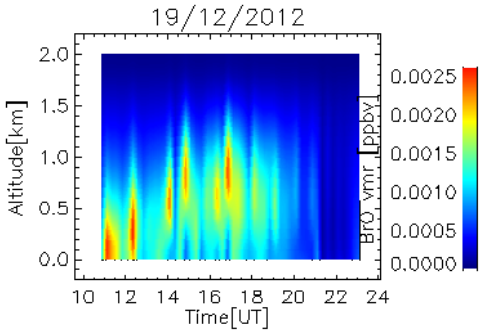

Fig. 5.17-3 Preliminary BrO profiles from MAX-DOAS measurements on 19 Dec 2012.

5.17.5 Time Line

It is planned to finish evaluating the MAX-DOAS data and having done radiative transfer modelling within half a year after the cruise. This then allows for the comparison on concentrations from the CE-DOAS measurements with the retrieved MAX-DOAS profiles.

5.18 Aerosol Sampling

(Hermann Bange, Alex Baker)

5.18.1 Overview

Ten aerosol samples were collected on a regular basis (48 h) between 04 and 24 December 2012 aboard R/V Meteor during M91. The filter samples were collected with an aerosol collector which was connected to a wind sector controller. The wind sector controller allowed pollution-free sampling by shutting off the aerosol collector when the wind was coming from the back of the ship. Thus sampling of pollution events caused by the plume of ship's engine were avoided. Sample positions are summarised in Table 5.18.

5.18.2 Measured Parameters

The aerosol samples will be analyses for their concentrations of soluble major cations (Na^+, Mg^{2+}, K^+, Ca^{2+}), aerosol trace metals (including Fe, Al, Mn, Ti and Zn), major anions (Cl^-, NO_3^-, SO_4^{2-}, Br^-, $C_2O_4^{2-}$), ammonium, total soluble nitrogen, soluble phosphate and soluble silicate.

5.18.3 Methods

All analytical methods to be employed are based on extraction of soluble aerosol components into aqueous solution, filtration and appropriate analysis. For major ions and total soluble nitrogen analysis the extraction solution is ultrapure water, while for the other species pH buffered solutions will be employed (pH 4.7 for trace metals, pH 7 for phosphate and silicate). Analysis of extract solutions will be done by ion chromatography (major ions), high temperature catalytic oxidation (total soluble nitrogen), inductively coupled plasma – optical emission spectrometry (trace metals) or spectrophotometry (phosphate and silicate). Full details of analytical methods can be found in Baker et al. (2007).

5.18.4 Time Line

The samples will be analysed within 1.5 years.

Tab. 5.18: List of aerosol samples during M91 (date and time are given in UTC).

Sample #	Start let S	Start long W	Start dd/mm	Start time	Stop let S	Stop long W	Stop dd/mm	Stop time
M91TM01	06°21.92’	81°25.82‘	04/12	23:47	08°06.64‘	80°04.05‘	06/12	23:18
M91TM02*	08°06.26‘	80°03.31‘	06/12	23:26	09°34.15‘	79°19.05‘	08/12	23:29
M91TM03	09°34.15‘	79°19.06‘	08/12	23:40	10°50.60‘	78°22.67‘	10/12	22:58
M91TM04	10°50.50‘	78°22.51‘	10/12	23:10	12°02.38‘	79°00.02‘	12/12	23:12
M91TM05	12°02.38‘	79°00.02‘	12/12	23:17	12°25.21‘	77°48.60‘	14/12	23:10
M91TM06	12°25.21‘	77°48.60‘	14/12	23:26	13°25.79‘	76°22.20‘	16/12	23:15
M91TM07	13°25.80‘	76°22.20‘	16/12	23:25	14°33.52‘	77°39.33‘	18/12	23:02
M91TM08	14°34.05‘	77°40.24‘	18/12	23:13	16°09.38‘	76°49‘55‘	20/12	23:18
M91TM09	16°09.32‘	76°49.39‘	20/12	23:38	15°32.42‘	75°37.36‘	22/12	23:27
M91TM10	15°32.42‘	75°37.36‘	22/12	23:35	14°22.49‘	76°15.10‘	24/12	23:05

*Collector was shut off from 07/12, ~12:00 to 07/12, ~21 .00 UTC because of a motor failure.

5.19 Expected Results

(H.W. Bange and the M91 Team)

M91 was the first comprehensive biogeochemical/atmospheric study in the upwelling region off Peru. When the complete set of results is available we expect to

- get a first comprehensive picture of the atmospheric trace gas distribution in the marine boundary layer and identify source regions,
- estimate the contribution of the atmospheric deposition of nutrients and trace metals to the ocean surface layer,
- get a first comprehensive picture of the distribution of dissolved trace gases in the upwelling area and identify hot spots of emissions,
- establish a new parameterization for the air/sea gas exchange which includes the effects of DOM in the sea surface microlayer,
- get a robust estimate of trace gas emissions from the coastal region off Peru and assess its global relevance (for this task we will also use trace gas data from the M90, M92 and M93 cruises in the upwelling and eastern tropical South Pacific Ocean),
- establish a budget for trace gases in the mixed layer by using an air/sea gas exchange parameterization, diapycnal fluxes into the mixed layer and upwelling velocities in order to identify missing sources or sinks,
- decipher the major production/consumption pathways of N_2O, halocarbons, DMS and other trace gases, and
- decipher the major nitrogen processes in the oxygen minimum zone and the upwelling off Peru.

All results will be published in international, high-ranking, open-access journals such as Biogeosciences (BG) and Atmospheric Chemistry and Physics (ACP). We may initiate a M91 joint BG/ACP special issue for M91.

6 Ship's Meteorological Station

(Bernd Frey)

On 01 December 2012 R/V Meteor left port of Callao and headed north for Transect A near Sechura Bay which is about 1000 km north of Callao. From 01 Dec to 04 Dec Meteor operated on the northeastern edge of a high-pressure ridge near the coast of Ecuador. At that time, the sky was mostly cloudy to overcast and rarely changed into scattered cloud cover. The southeast trade wind was a constant mild to moderate breeze and also the swell from south to southwest direction was comfortable. From 05 Dec to 08 Dec a weak trough appeared parallel to the coast where the ship operated. Visibility was good up to that point. During the night of 06/07 Dec the visibility steadily decreased and after midnight the weather became foggy. On the morning of 07 Dec the visibility was in the medium range and changed into fog during the forenoon. At noon the fog disappeared and the visibility became high again. On 08 Dec the visibility decreased to a medium range but was high again on 09 Dec. During that time the sky was mostly cloudy. Wind was at 3-4 Bft and came from southeasterly direction. At the afternoon of the 09 Dec wind changed into a fresh breeze from southeast. Several stormy gusts occurred at that afternoon, too. From 10 to 15 Dec Meteor moved into the northeastern area of a high pressure zone. Visibility became low again and on the morning of 11 Dec the weather changed into fog for about one hour. During these days usually the sky was overcast at first and changed into a scattered cloud cover on the afternoon. On 10 and 11 Dec the wind decreased from 5-6 Bft in the morning to 1 Bft at the forenoon of 11 Dec. However, during the afternoon of the same day the wind force increased to 4 Bft which was the typical force during that cruise. On the 14 Dec the wind increased to 5 Bft but already on the next morning it decreased to a light breeze of 1-2 Bft. During the 15 Dec the wind remained as a light breeze. Sea state was only 1-1.5 m during these days. During 16 Dec a trough from northwest reached into the operation area. Between midnight and the morning of the 16 Dec several fog banks crossed the ship's cruise track. During the night from 16 to 17 Dec stormy gusts appeared for the last time during M91. Until forenoon the wind calmed down to a fresh southeasterly breeze. Eventually after a short rain shower at the morning of the 18 Dec the visibility became clear again. During the same time a cyclone developed near southern Chile and caused higher long waves in the ship's operation area on 20 Dec. For that reason the sea state rose up to 3 m high instead of the usual 1.5 m which was usually encountered during cruise. Already on the 21 Dec high-pressure influence became stronger again and so the swell decreased until 22 Dec to comfortable 1-1.5 meters. The wind which was still a strong wind on the day before and calmed down to a light air during the forenoon of the 22 Dec. However, within the following 12 hours it increased to the typical 4-5 Bft again. On the forenoon of 25 Dec there was only a light breeze from northerly directions with a swell of 0.5 to 1 m from southwest. On the way back along the coast to Callao the wind was constant at 4-5 Bft between 23 and 26 Dec. The wind direction however slightly changed to a more southerly direction compared to the previous encountered southeasterly direction. As expected the visibility

decreased to a medium range at the night from 25 to 26 Dec on the way through the Bay of Pisco. On the morning of the 26 Dec the cruise M91 was finished in the harbour of Callao.

Brief summary of the meteorological conditions during M91:

- The wind was between 3-5 Bft most of the time
- The sea state was between 1.5 to 2 meters most of the time
- The visibility range was usually between 10 to 20 km
- The cloud cover was most of the time between 5-8 eighth and consisted of medium/high and high clouds

Group photo: Participants of M91

From the left: Hermann Bange, Steffen Fuhlbrügge, Damian Arevalo, Avy Bernales, Bettina Derstroff, Daniel Kiefhaber, Violeta Leon, Verena Ihnenfeld, Kristian Rother, Georgina Flores, Maike Peters, Sebastian Flöter, Leila Nagel, Wei Song, Johannes Lampel, Stefan Raimund, Luisa Galgani, Patrick Veres, Annie Bourbonnais, Matthias Krüger, Kerstin Nachtigall, Ingo Weinberg, Tina Baustian, Tim Fischer, Helmke Hepach, Jon Roa, Annette Kock, Natascha Martogli and Joel Craig.

7 Station List M91

7.1 Station List: CTD/RO, MSS, Zodiac

24h stations are marked in bold.

Stat#-Cast#	Transect	Date, UTC	Time, UTC	Position, Lat	Position, Lon	Water depth, m	Gear	CTD/RO depth, m	Remarks
M910/1712-1		02/12/2012	13:13	9° 3.61' S	79° 58.82' W	708.1	CTD/RO	404	test station
M910/1712-2		02/12/2012	13:44	9° 3.62' S	79° 58.76' W	583.4	MSS		test station
M910/1713-1	A	03/12/2012	12:23	5° 0.01' S	82° 0.01' W	5289.5	CTD/RO	2005	
M910/1713-2	A	03/12/2012	13:51	5° 0.11' S	81° 59.98' W	5288.8	MSS		
M910/1713-3	A	03/12/2012	15:44	4° 59.99' S	82° 0.02' W	5290	CTD/RO	199	
M910/1713-4	A	03/12/2012	16:07	4° 59.98' S	82° 0.02' W	5289.2	ZODIAC		
M910/1714-1	A	03/12/2012	18:34	5° 0.00' S	81° 49.81' W	4535.7	CTD/RO	2006	
M910/1715-1	A	03/12/2012	21:44	5° 0.01' S	81° 40.23' W	2837.6	CTD/RO	2008	
M910/1715-2	A	03/12/2012	23:11	5° 0.02' S	81° 40.21' W	2828.9	MSS		
M910/1715-3	A	04/12/2012	01:03	5° 0.0 0' S	81° 40.22' W	2834.6	CTD/RO	217	
M910/1716-1	A	04/12/2012	03:19	4° 59.98' S	81° 30.02' W	1494.6	CTD/RO	1157	
M910/1717-1	A	04/12/2012	06:03	5° 0.01' S	81° 19.81' W	117.5	CTD/RO	107	
M910/1717-2	A	04/12/2012	06:41	5° 0.03' S	81° 19.81' W	115.9	MSS		
M910/1718-1	A	04/12/2012	09:02	5° 0.00' S	81° 10.19' W	27	CTD/RO	25	
M910/1719-1	B	04/12/2012	16:13	6° 11.40' S	81° 8.41' W	313.6	CTD/RO	302	
M910/1719-2	B	04/12/2012	16:43	6° 11.52' S	81° 8.44' W	333.5	MSS		
M910/1719-3	B	04/12/2012	18:06	6° 13.72' S	81° 9.24' W	1201.7	ZODIAC		
M910/1720-1	B	04/12/2012	20:17	6° 16.80' S	81° 17.41' W	1829.3	CTD/RO	1756	
M910/1720-2	B	04/12/2012	21:31	6° 16.80' S	81° 17.41' W	1828.5	ZODIAC		
M910/1721-1	B	04/12/2012	23:41	6° 21.92' S	81° 25.81' W	2644.1	CTD/RO	1988	
M910/1721-2	B	05/12/2012	01:05	6° 22.02' S	81° 25.84' W	2652	MSS		
M910/1721-3	B	05/12/2012	03:03	6° 21.93' S	81° 25.81' W	2643.2	CTD/RO	152	
M910/1722-1	B	05/12/2012	05:10	6° 26.99' S	81° 34.20' W	3662.6	CTD/RO	2006	
M910/1723-1	B	05/12/2012	08:27	6° 32.39' S	81° 42.59' W	5669	CTD/RO	2009	
M910/1724-1	B	05/12/2012	11:11	6° 37.18' S	81° 49.79' W	5398	CTD/RO	2000	

Stat#-Cast#	Transect	Date, UTC	Time, UTC	Position, Lat	Position, Lon	Water depth, m	Gear	CTD/RO depth, m	Remarks
M910/1724-2	B	05/12/2012	12:35	6° 37.20' S	81° 49,80' W	5393.5	MSS		
M910/1724-3	B	05/12/2012	14:30	6° 37.19' S	81° 49,81' W	5396.4	CTD/RO	152	
M910/1724-4	B	05/12/2012	14:51	6° 37.19' S	81° 49.81' W	5396.7	ZODIAC		
M910/1725-1	C	06/12/2012	02:18	8° 37.82' S	80° 59.97' W	5954.9	CTD/RO	2008	
M910/1725-2	C	06/12/2012	03:43	8° 37.87' S	81° 0.02' W	5949.4	MSS		
M910/1725-3	C	06/12/2012	05:46	8° 37.81' S	81° 0.02' W	5951.8	CTD/RO	150	
M910/1726-1	C	06/12/2012	09:50	8° 28.18' S	80° 42.61' W	2984	CTD/RO	2008	
M910/1727-1	C	06/12/2012	14:27	8° 18.61' S	80° 24.59' W	854.1	CTD/RO	843	
M910/1727-2	C	06/12/2012	15:18	8° 18.67' S	80° 24.62' W	856.3	MSS		
M910/1727-3	C	06/12/2012	17:03	8° 18.61' S	80° 24.61' W	856.9	CTD/RO	150	
M910/1727-4	C	06/12/2012	17:31	8° 18.62' S	80° 24.61' W	854.7	ZODIAC		
M910/1728-1	C	06/12/2012	21:33	8° 8.46' S	80° 7.20' W	171.9	ZODIAK		
M910/1728-2	C	06/12/2012	22:14	8° 8.40' S	80° 7.19' W	171.7	CTD/RO	150	
M910/1729-1	C	07/12/2012	01:57	7° 58.79' S	79° 49.80' W	137.5	CTD/RO	131	
M910/1729-2	C	07/12/2012	02:24	7° 58.82' S	79° 49.82' W	138.2	MSS		
M910/1730-1	C	07/12/2012	06:25	7° 49.66' S	79° 33.23' W	55.8	CTD/RO	35	
M910/1731-1	D	07/12/2012	15:20	9° 11.39' S	78° 40.21' W	66.3	CTD/RO	58	
M910/1732-1	D	07/12/2012	19:07	9° 19.79' S	78° 58.19' W	121.8	CTD/RO	110	
M910/1732-2	D	07/12/2012	19:31	9° 19.79' S	78° 58.19' W	121.8	ZODIAC		
M910/1733-1	**D**	**07/12/2012**	**23:27**	**9° 28.80' S**	**79° 16.80' W**	**156.1**	**CTD/RO**	**151**	
M910/1733-2	**D**	**07/12/2012**	**23:56**	**9° 28.81' S**	**79° 16.81' W**	**155.9**	**MSS**		
M910/1733-3	**D**	**08/12/2012**	**03:58**	**9° 29.52' S**	**79° 17.07' W**	**156.5**	**MSS**		
M910/1733-4	**D**	**08/12/2012**	**08:03**	**9° 30.24' S**	**79° 17.39' W**	**156.4**	**MSS**		
M910/1733-5	**D**	**08/12/2012**	**10:49**	**9° 31.26' S**	**79° 17.89' W**	**154.2**	**ZODIAC**		
M910/1733-6	**D**	**08/12/2012**	**11:33**	**9° 31.26' S**	**79° 17.89' W**	**156**	**CTD/RO**	**150**	
M910/1733-7	**D**	**08/12/2012**	**11:58**	**9° 31.27' S**	**79° 17.89' W**	**155.3**	**MSS**		
M910/1733-8	**D**	**08/12/2012**	**16:00**	**9° 31.85' S**	**79° 18.16' W**	**153.8**	**MSS**		
M910/1733-9	**D**	**08/12/2012**	**19:15**	**9° 32.75' S**	**79° 18.43' W**	**155.2**	**ZODIAC**		
M910/1733-10	**D**	**08/12/2012**	**20:06**	**9° 32.81' S**	**79° 18.44' W**	**154.9**	**MSS**		
M910/1733-11	**D**	**08/12/2012**	**20:45**	**9° 33.67' S**	**79° 18.77' W**	**153.7**	**ZODIAC**		
M910/1733-12	**D**	**08/12/2012**	**22:30**	**9° 33.68' S**	**79° 18.78' W**	**153.8**	**MSS**		
M910/1733-13	**D**	**08/12/2012**	**23:14**	**9° 34.15' S**	**79° 19.06' W**	**152.8**	**CTD/RO**	**150**	
M910/1734-1	D	09/12/2012	02:23	9° 37.19' S	79° 34.80' W	393.2	CTD/RO	388	

Stat#-Cast#	Transect	Date, UTC	Time, UTC	Position, Lat	Position, Lon	Water depth, m	Gear	CTD/RO depth, m	Remarks
M910/1735-1	D	09/12/2012	06:21	9° 46.18' S	79° 52.83' W	1638.2	CTD/RO	1606	
M910/1736-1	D	09/12/2012	11:25	9° 55.82' S	80° 13.79' W	6342.9	CTD/RO	2006	
M910/1736-2	D	09/12/2012	12:58	9° 55.82' S	80° 13.83' W	6342.9	MSS		
M910/1736-3	D	09/12/2012	14:38	9° 57.28' S	80° 14.77' W	6338.1	CTD/RO	198	
M910/1736-4	D	09/12/2012	15:05	9° 57.28' S	80° 14.77' W	6337	ZODIAC		
M910/1737-1	E	10/12/2012	01:26	11° 28.20' S	79° 25.80' W	5890	CTD/RO	2005	
M910/1737-2	E	10/12/2012	02:48	11° 28.24' S	79° 25.79' W	5891.2	MSS		
M910/1737-3	E	10/12/2012	04:43	11° 29.88' S	79° 25.50' W	5878.9	CTD/RO	125	
M910/1738-1	E	10/12/2012	08:06	11° 17.39' S	79° 8.39' W	3950.4	CTD/RO	2008	
M910/1739-1	E	10/12/2012	12:45	11° 7.19' S	78° 51.00' W	2262.3	CTD/RO	2006	
M910/1739-2	E	10/12/2012	14:13	11° 7.25' S	78° 50.97' W	2260.8	MSS		
M910/1739-3	E	10/12/2012	15:25	11° 8.18' S	78° 50.25' W	2245.9	CTD/RO	151	
M910/1739-4	E	10/12/2012	15:49	11° 8.18' S	78° 50.25' W	2246.5	ZODIAC		
M910/1740-1	E	10/12/2012	19:45	10° 56.99' S	78° 33.59' W	1078.2	CTD/RO	1065	
M910/1740-2	E	10/12/2012	20:36	10° 56.99' S	78° 33.60' W	1079.3	ZODIAC		
M910/1741-1	E	11/12/2012	00:33	10° 46.81' S	78° 16.20' W	310.4	CTD/RO	301	
M910/1741-2	E	11/12/2012	01:05	10° 46.82' S	78° 16.21' W	309.9	MSS		
M910/1742-1	E	11/12/2012	05:20	10° 37.50' S	78° 0.29' W	107.8	CTD/RO	99	
M910/1743-1	F	11/12/2012	15:46	12° 0.49' S	77° 13.84' W	56.7	CTD/RO	52	
M910/1743-2	F	11/12/2012	16:04	12° 0.49' S	77° 13.84' W	55.5	ZODIAC		
M910/1744-1	F	11/12/2012	17:43	12° 3.08' S	77° 18.21' W	100.7	CTD/RO	92	
M910/1744-2	F	11/12/2012	18:05	12° 3.08' S	77° 18.21' W	101.4	ZODIAC		
M910/1745-1	F	11/12/2012	19:24	12° 2.39' S	77° 22.21' W	115.9	CTD/RO	109	
M910/1745-2	F	11/12/2012	19:46	12° 2.39' S	77° 22.21' W	116.6	ZODIAC		
M910/1746-1	F	11/12/2012	21:29	12° 2.39' S	77° 29.41' W	142	CTD/RO	139	
M910/1746-2	F	11/12/2012	21:54	12° 2.42' S	77° 29.42' W	142.2	MSS		
M910/1746-3	F	11/12/2012	22:30	12° 2.95' S	77° 29.65' W	143.8	ZODIAC		
M910/1747-1	F	12/12/2012	00:30	12° 2.39' S	77° 39.00' W	180.3	CTD/RO	170	
M910/1748-1	F	12/12/2012	02:48	12° 2.37' S	77° 49.21' W	822.7	CTD/RO	822	
M910/1748-2	F	12/12/2012	03:37	12° 2.40' S	77° 49.19' W	809.7	MSS		
M910/1749-1	F	12/12/2012	07:23	12° 2.39' S	77° 58.80' W	1708.1	CTD/RO	1695	
M910/1749-2	F	12/12/2012	08:44	12° 2.41' S	77° 58.80' W	1707.5	MSS		
M910/1750-1	F	12/12/2012	14:44	12° 2.38' S	78° 30.02' W	3078.9	CTD/RO	2008	

Stat#-Cast#	Transect	Date, UTC	Time, UTC	Position, Lat	Position, Lon	Water depth, m	Gear	CTD/RO depth, m	Remarks
M910/1750-2	F	12/12/2012	16:07	12° 2.44' S	78° 30.01' W	3078.3	MSS		
M910/1750-3	F	12/12/2012	17:37	12° 3.79' S	78° 29.65' W	3069.4	ZODIAC		
M910/1751-1	F	12/12/2012	23:01	12° 2.42' S	79° 0.05' W	6072.4	CTD/RO	2006	
M910/1751-2	F	13/12/2012	00:34	12° 2.41' S	79° 0.02' W	6080.4	MSS		
M910/1751-3	F	13/12/2012	02:22	12° 4.13' S	79° 0.26' W	5977.1	CTD/RO	174	
M910/1752-1	**G**	**13/12/2012**	**08:24**	**12° 55.21' S**	**78° 42.02' W**	**5044.4**	**CTD/RO**	**5012**	
M910/1752-2	**G**	**13/12/2012**	**11:34**	**12° 55.20' S**	**78° 42.00' W**	**5039.7**	**ZODIAC**		
M910/1752-3	**G**	**13/12/2012**	**12:04**	**12° 55.23' S**	**78° 42.00' W**	**5039.2**	**MSS**		
M910/1752-4	**G**	**13/12/2012**	**13:33**	**12° 56.94' S**	**78° 41.44' W**	**4949.6**	**CTD/RO**	**174**	
M910/1752-5	**G**	**13/12/2012**	**14:05**	**12° 56.96' S**	**78° 41.43' W**	**4950.4**	**ZODIAC**		
M910/1752-6	**G**	**13/12/2012**	**18:38**	**12° 57.03' S**	**78° 41.43' W**	**4946.6**	**MSS**		
M910/1752-7	**G**	**13/12/2012**	**20:08**	**12° 59.80' S**	**78° 40.98' W**	**4962.8**	**ZODIAC**		
M910/1752-8	**G**	**13/12/2012**	**21:21**	**12° 55.20' S**	**78° 42.03' W**	**5035.6**	**CTD/RO**	**2006**	
M910/1752-9	**G**	**13/12/2012**	**22:41**	**12° 55.20' S**	**78° 42.03' W**	**5047.3**	**ZODIAC**		
M910/1752-10	**G**	**14/12/2012**	**00:30**	**12° 55.23' S**	**78° 42.03' W**	**5036.7**	**MSS**		
M910/1752-12	**G**	**14/12/2012**	**07:21**	**12° 57.73' S**	**78° 42.63' W**	**4960.2**	**CTD/RO**	**2005**	
M910/1753-1	G	14/12/2012	12:00	12° 44.99' S	78° 24.01' W	5940	CTD/RO	2007	
M910/1753-2	G	14/12/2012	13:19	12° 45.00' S	78° 24.01' W	5943.6	ZODIAC		
M910/1754-1	G	14/12/2012	17:21	12° 34.79' S	78° 6.61' W	3052	CTD/RO	2010	
M910/1754-2	G	14/12/2012	18:57	12° 34.79' S	78° 6.61' W	3046.9	ZODIAC		
M910/1755-1	G	14/12/2012	22:56	12° 25.21' S	77° 48.62' W	1100.9	ZODIAC		
M910/1755-2	G	14/12/2012	23:43	12° 25.21' S	77° 48.61' W	1102.2	CTD/RO	1088	
M910/1755-3	G	15/12/2012	00:42	12° 25.23' S	77° 48.60' W	1099.7	MSS		
M910/1755-4	G	15/12/2012	02:24	12° 26.49' S	77° 49.03' W	1158.4	CTD/RO	181	
M910/1756-1	G	15/12/2012	06:28	12° 15.01' S	77° 31.21' W	202	CTD/RO	194	
M910/1756-2	G	15/12/2012	07:06	12° 15.03' S	77° 31.21' W	202.5	MSS		
M910/1757-1	G	15/12/2012	10:02	12° 6.93' S	77° 17.50' W	96	CTD/RO	88	
M910/1758-1	H	15/12/2012	12:55	12° 16.31' S	77° 1.14' W	70.7	CTD/RO	67	
M910/1758-2	H	15/12/2012	13:13	12° 16.31' S	77° 1.14' W	70.2	ZODIAC		
M910/1759-1	H	15/12/2012	17:26	12° 33.01' S	76° 50.39' W	104.3	CTD/RO	98	
M910/1759-2	H	15/12/2012	17:50	12° 33.04' S	76° 50.37' W	103.4	MSS		
M910/1759-3	H	15/12/2012	18:28	12° 33.95' S	76° 50.25' W	104.5	ZODIAC		
M910/1760-1	H	16/12/2012	12:47	12° 50.41' S	76° 40.80' W	101.9	CTD/RO	98	

Stat#-Cast#	Transect	Date, UTC	Time, UTC	Position, Lat	Position, Lon	Water depth, m	Gear	CTD/RO depth, m	Remarks
M910/1760-2	H	16/12/2012	13:09	12° 50.44' S	76° 40.78' W	102	MSS		
M910/1760-3	H	16/12/2012	13:48	12° 51.27' S	76° 40.66' W	108	ZODIAC		
M910/1761-1	H	16/12/2012	17:36	13° 8.42' S	76° 31.81' W	98.4	CTD/RO	90	
M910/1761-2	H	16/12/2012	17:58	13° 8.40' S	76° 31.80' W	97.3	ZODIAC		
M910/1761-3	H	16/12/2012	18:30	13° 8.40' S	76° 31.80' W	96.8	ZODIAC		
M910/1762-1	H	16/12/2012	22:44	13° 25.78' S	76° 22.19' W	85.4	ZODIAC		
M910/1762-2	H	16/12/2012	23:17	13° 25.79' S	76° 22.20' W	86	CTD/RO	81	
M910/1762-3	H	16/12/2012	23:38	13° 25.81' S	76° 22.24' W	86.3	MSS		
M910/1763-1	I	17/12/2012	03:33	13° 56.96' S	76° 34.23' W	252.6	CTD/RO	245	
M910/1763-2	I	17/12/2012	04:02	13° 57.04' S	76° 34.22' W	254.9	MSS		
M910/1764-1	**I**	**17/12/2012**	**08:34**	**14° 7.23' S**	**76° 52.23' W**	**0**	**CTD/RO**	**2252**	
M910/1764-2	**I**	**17/12/2012**	**10:16**	**14° 7.27' S**	**76° 52.26' W**	**2270.9**	**MSS**		
M910/1764-3	**I**	**17/12/2012**	**11:49**	**14° 8.77' S**	**76° 53.89' W**	**2622.4**	**CTD/RO**	**200**	
M910/1764-4	**I**	**17/12/2012**	**12:11**	**14° 8.77' S**	**76° 53.89' W**	**2624.1**	**ZODIAC**		
M910/1764-5	**I**	**17/12/2012**	**16:02**	**14° 8.79' S**	**76° 53.93' W**	**2630.5**	**MSS**		
M910/1764-6	**I**	**17/12/2012**	**17:38**	**14° 11.11' S**	**76° 55.95' W**	**3108**	**ZODIAC**		
M910/1764-7	**I**	**17/12/2012**	**18:05**	**14° 11.10' S**	**76° 55.99' W**	**3112.1**	**ZODIAC**		
M910/1764-8	**I**	**17/12/2012**	**20:33**	**14° 11.10' S**	**76° 55.99' W**	**3114.4**	**CTD/RO**	**2007**	
M910/1764-9	**I**	**17/12/2012**	**22:00**	**14° 11.10' S**	**76° 55.99' W**	**3113.1**	**ZODIAK**		
M910/1764-10	**I**	**17/12/2012**	**22:30**	**14° 11.11' S**	**76° 56.01' W**	**3120.1**	**MSS**		
M910/1764-11	**I**	**18/12/2012**	**04:00**	**14° 12.57' S**	**76° 57.42' W**	**3415.1**	**MSS**		
M910/1764-12	**I**	**18/12/2012**	**07:03**	**14° 14.36' S**	**76° 58.78' W**	**3677.5**	**CTD/RO**	**2009**	
M910/1765-1	I	18/12/2012	12:00	14° 16.79' S	77° 10.21' W	6545.8	CTD/RO	2007	
M910/1765-2	I	18/12/2012	13:20	14° 16.79' S	77° 10.21' W	4707.6	ZODIAC		
M910/1766-1	I	18/12/2012	17:27	14° 26.99' S	77° 28.23' W	4621.6	CTD/RO	2007	
M910/1766-2	I	18/12/2012	18:58	14° 27.07' S	77° 28.33' W	4624.3	MSS		
M910/1766-3	I	18/12/2012	20:31	14° 29.23' S	77° 29.95' W	4604.2	CTD/RO	175	
M910/1766-4	I	18/12/2012	20:56	14° 29.23' S	77° 29.95' W	4596.7	ZODIAC		
M910/1767-1	I	19/12/2012	00:23	14° 37.20' S	77° 45.60' W	4271.5	CTD/RO	2006	failure: bottles not closed
M910/1767-2	I	19/12/2012	02:19	14° 37.20' S	77° 45.60' W	4276.7	CTD/RO	2007	
M910/1768-1	I	19/12/2012	06:55	14° 46.20' S	78° 1.80' W	4177.5	CTD/RO	2007	
M910/1768-2	I	19/12/2012	08:30	14° 46.40' S	78° 1.94' W	4175.1	MSS		

Stat#-Cast#	Transect	Date, UTC	Time, UTC	Position, Lat	Position, Lon	Water depth, m	Gear	CTD/RO depth, m	Remarks
M910/1768-3	I	19/12/2012	10:05	14° 48.04' S	78° 2.65' W	4142.7	CTD/RO	176	
M910/1769-1	Ia	19/12/2012	13:53	15° 2.84' S	77° 47.38' W	3955.4	CTD/RO	1003	
M910/1769-2	Ia	19/12/2012	14:46	15° 2.93' S	77° 47.39' W	3969.4	MSS		
M910/1769-3	Ia	19/12/2012	16:17	15° 4.18' S	77° 46.72' W	3958.9	ZODIAC		
M910/1770-1	Ia	19/12/2012	20:35	15° 19.67' S	77° 32.08' W	3576.6	ZODIAC		
M910/1770-2	Ia	19/12/2012	21:07	15° 19.68' S	77° 32.02' W	3591.5	CTD/RO	1002	
M910/1770-3	Ia	19/12/2012	22:11	15° 19.70' S	77° 32.03' W	3576.1	MSS		
M910/1770-4	Ia	19/12/2012	23:41	15° 21.20' S	77° 32.78' W	3588.1	CTD/RO	200	
M910/1771-1	Ia	20/12/2012	03:30	15° 36.53' S	77° 18.07' W	3012.4	CTD/RO	1003	
M910/1771-2	Ia	20/12/2012	04:16	15° 36.58' S	77° 18.06' W	3009.8	MSS		
M910/1772-1	Ia	20/12/2012	09:40	15° 53.48' S	77° 3.45' W	2669.7	CTD/RO	1004	
M910/1772-2	Ia	20/12/2012	10:21	15° 53.52' S	77° 3.45' W	2670	MSS		failure
M910/1772-3	Ia	20/12/2012	10:58	15° 54.15' S	77° 3.56' W	2642.1	ZODIAC		
M910/1772-4	Ia	20/12/2012	11:32	15° 54.21' S	77° 3.62' W	2643.6	MSS		
M910/1773-1	**J**	**20/12/2012**	**16:19**	**16° 10.71' S**	**76° 48.25' W**	**2843**	**MSS**		
M910/1773-2	**J**	**20/12/2012**	**17:56**	**16° 9.49' S**	**76° 48.27' W**	**2827**	**CTD/RO**	**2013**	
M910/1773-3	**J**	**20/12/2012**	**20:32**	**16° 9.38' S**	**76° 49.28' W**	**2810.4**	**CTD/RO**	**181**	
M910/1773-4	**J**	**20/12/2012**	**23:33**	**16° 9.36' S**	**76° 49.47' W**	**2770.9**	**MSS**		
M910/1773-5	**J**	**21/12/2012**	**04:00**	**16° 10.48' S**	**76° 48.46' W**	**2823.6**	**CTD/RO**	**--**	**stat. cancelled: heavy swell**
M910/1774-1	J	21/12/2012	19:40	16° 1.15' S	76° 30.14' W	3213.8	CTD/RO	2010	
M910/1774-2	J	21/12/2012	21:15	16° 1.14' S	76° 30.73' W	3223.9	MSS		
M910/1774-3	J	21/12/2012	22:55	16° 3.29' S	76° 31.43' W	3205.9	CTD/RO	203	
M910/1775-1	J	22/12/2012	02:35	15° 50.96' S	76° 12.08' W	3564.9	CTD/RO	2011	
M910/1775-2	J	22/12/2012	04:06	15° 50.99' S	76° 12.15' W	3563.8	MSS		
M910/1775-3	J	22/12/2012	05:54	15° 52.49' S	76° 12.17' W	3544.1	CTD/RO	176	
M910/1776-1	J	22/12/2012	09:30	15° 41.40' S	75° 54.02' W	5105.1	CTD/RO	2009	
M910/1776-2	J	22/12/2012	10:58	15° 41.46' S	75° 54.01' W	6692.6	MSS		
M910/1776-3	J	22/12/2012	12:23	15° 42.79' S	75° 53.97' W	7204.8	ZODIAC		
M910/1776-4	J	22/12/2012	12:54	15° 42.79' S	75° 53.97' W	5061.9	CTD/RO	199	
M910/1777-1	**J**	**22/12/2012**	**16:40**	**15° 31.17' S**	**75° 36.02' W**	**2230.9**	**CTD/RO**	**2010**	
M910/1777-2	**J**	**22/12/2012**	**18:05**	**15° 31.17' S**	**75° 36.01' W**	**2229.8**	**ZODIAC**		

Stat#-Cast#	Transect	Date, UTC	Time, UTC	Position, Lat	Position, Lon	Water depth, m	Gear	CTD/RO depth, m	Remarks
M910/1777-3	**J**	**22/12/2012**	**18:34**	**15° 31.19' S**	**75° 36.03' W**	**2233.6**	**MSS**		
M910/1777-4	**J**	**22/12/2012**	**20:05**	**15° 32.44' S**	**75° 36.84' W**	**2546.9**	**CTD/RO**	**200**	
M910/1777-5	**J**	**22/12/2012**	**20:31**	**15° 32.44' S**	**75° 36.84' W**	**2546.4**	**ZODIAC**		
M910/1777-6	**J**	**23/12/2012**	**00:31**	**15° 32.46' S**	**75° 37.36' W**	**2607.9**	**MSS**		
M910/1777-7	**J**	**23/12/2012**	**04:30**	**15° 33.57' S**	**75° 37.76' W**	**2791.3**	**CTD/RO**	**2009**	
M910/1777-8	**J**	**23/12/2012**	**06:34**	**15° 33.65' S**	**75° 37.77' W**	**2793.5**	**MSS**		
M910/1777-9	**J**	**23/12/2012**	**12:34**	**15° 35.19' S**	**75° 38.24' W**	**3137.7**	**MSS**		
M910/1777-10	**J**	**23/12/2012**	**13:56**	**15° 36.42' S**	**75° 38.60' W**	**3375.6**	**ZODIAC**		
M910/1777-11	**J**	**23/12/2012**	**14:57**	**15° 36.42' S**	**75° 38.60' W**	**3376.1**	**CTD/RO**	**2011**	
M910/1778-1	J	23/12/2012	20:01	15° 22.76' S	75° 19.91' W	276.3	CTD/RO	270	
M910/1778-2	J	23/12/2012	20:39	15° 22.83' S	75° 20.04' W	268.7	MSS		
M910/1778-3	J	23/12/2012	21:33	15° 23.64' S	75° 21.20' W	164.3	ZODIAC		
M910/1778-4	J	23/12/2012	22:54	15° 23.40' S	75° 21.58' W	138.1	CTD/RO	133	

24h stations are marked in bold.

7.2 Station List: Sampled parameters

Table Legend:
Nut. stands for dissolved nutrients (nitrate, nitrite, ammonium, silicate and phosphate)

(1) U, Utermöhl; C, S, Ca and Si isotopes; DIC (diss. inorganic carbon); TA (total alkalinity) by IMARPE
(2) pH measurements by IMARPE
(3) Helium isotope by U Bremen
(4) VOCs by MPI Mainz
(5) DMS, DMSP, DMSO by GEOMAR
(6) N_2O by GEOMAR
(7) N_2 fixation, N_2O production, NH_2OH production by U Kiel
(8) C, CH_4; O, NH_2OH; H, N_2H_4 by GEOMAR
(9) DIN isotopes (^{15}N, ^{18}O), $DO^{15}N$, N_2O isotopomers, $PO^{15}N$, N_2/Ar by U Mass.
(10) DOM from CTD by GEOMAR
(11) DOM in surface microlayer by GEOMAR
(12) Chl. a, flow cytometry by GEOMAR, U Kiel
(13) DNA/RNA filtration by GEOMAR, U Kiel
(14) Halocarbons by GEOMAR
(15) inorganic halogens, POBr and POI by GEOMAR/TU Braunschweig
(16) Halocarbons isotopes by U Hamburg/IOW

24h stations are marked in bold.

Stat#-Cast#	Tran-sect	Gear	CTD/RO m	Nut., O_2	(1)	(2)	(3)	(4)	(5)	(6)	(7)	(8)	(9)	(10)	(11)	(12)	(13)	(14)	(15)	(16)
M910/1713-1	A	CTD/RO	2005	X		X		X	X	X	X		X	X		X				
M910/1713-3	A	CTD/RO	199	X		X	X	X	X	X	X		X	X		X				
M910/1713-4	A	ZODIAC													X					
M910/1714-1	A	CTD/RO	2006	X		X	X													
M910/1715-1	A	CTD/RO	2008	X		X		X		X			X							
M910/1715-3	A	CTD/RO	217	X		X	X	X	X	X			X				X			
M910/1716-1	A	CTD/RO	1157	X		X	X													
M910/1717-1	A	CTD/RO	107	X		X	X			X			X							
M910/1718-1	A	CTD/RO	25	X		X	X													

Stat#-Cast#	Tran-sect	Gear	CTD/RO m	Nut., O_2	(1)	(2)	(3)	(4)	(5)	(6)	(7)	(8)	(9)	(10)	(11)	(12)	(13)	(14)	(15)	(16)
M910/1719-1	B	CTD/RO	302	X		X	X	X	X	X	X		X			X				
M910/1719-3	B	ZODIAC													X					
M910/1720-1	B	CTD/RO	1756	X		X	X							X						
M910/1720-2	B	ZODIAC													X					
M910/1721-1	B	CTD/RO	1988	X		X				X			X							
M910/1721-3	B	CTD/RO	152	X		X	X	X	X	X			X			X				
M910/1722-1	B	CTD/RO	2006	X		X														
M910/1723-1	B	CTD/RO	2009	X		X														
M910/1724-1	B	CTD/RO	2000	X		X				X	X		X	X						
M910/1724-3	B	CTD/RO	152	X		X	X	X	X	X	X		X	X		X				
M910/1724-4	B	ZODIAC													X					
M910/1725-1	C	CTD/RO	2008	X		X	X		X	X	X	O	X			X	X			
M910/1725-3	C	CTD/RO	150	X		X	X	X	X	X	X	O	X			X				
M910/1726-1	C	CTD/RO	2008	X		X														
M910/1727-1	C	CTD/RO	843	X		X			X	X		O	X	X		X		X		
M910/1727-3	C	CTD/RO	150	X		X	X	X		X		O	X	X		X		X		
M910/1727-4	C	ZODIAC													X					
M910/1728-1	C	ZODIAC													X					
M910/1728-2	C	CTD/RO	150	X		X	X			X										
M910/1729-1	C	CTD/RO	131	X		X	X	X	X	X	X		X			X				
M910/1730-1	C	CTD/RO	35	X		X	X			X		O	X	X						
M910/1731-1	D	CTD/RO	58	X	U	X	X	X	X	X	X	O	X			X				
M910/1732-1	D	CTD/RO	110	X	U	X	X							X						
M910/1732-2	D	ZODIAC													X					
M910/1733-1	D	CTD/RO	151	X	U	X		X	X	X			X	X		X				X
M910/1733-5	D	ZODIAC													X					
M910/1733-6	D	CTD/RO	150	X		X	X	X					X	X						X
M910/1733-9	D	ZODIAC								X										
M910/1733-11	D	ZODIAC													X					
M910/1733-13	D	CTD/RO	150	X		X		X	X				X			X				X
M910/1734-1	D	CTD/RO	388	X	U	X	X	X												
M910/1735-1	D	CTD/RO	1606	X	U	X	X													
M910/1736-1	D	CTD/RO	2006	X		X				X	X	O	X	X		X		X		X

Stat#-Cast#	Tran-sect	Gear	CTD/RO m	Nut., O_2	(1)	(2)	(3)	(4)	(5)	(6)	(7)	(8)	(9)	(10)	(11)	(12)	(13)	(14)	(15)	(16)
M910/1736-3	D	CTD/RO	198	X		X	X	X	X	X	X	O	X	X				X		
M910/1736-4	D	ZODIAC													X					
M910/1737-1	E	CTD/RO	2005	X		X		X	X	X	X	H	X	X		X	X	X	X	
M910/1737-3	E	CTD/RO	125	X		X	X	X		X	X	H	X	X		X		X	X	
M910/1738-1	E	CTD/RO	2008	X		X	X													
M910/1739-1	E	CTD/RO	2006	X		X		X	X	X			X			X		X		
M910/1739-3	E	CTD/RO	151	X		X				X			X			X	X	X		
M910/1739-4	E	ZODIAC								X										
M910/1740-1	E	CTD/RO	1065	X		X	X	X												
M910/1740-2	E	ZODIAC													X					
M910/1741-1	E	CTD/RO	301	X		X	X	X	X	X			X			X		X		
M910/1742-1	E	CTD/RO	99	X		X	X				X									
M910/1743-1	F	CTD/RO	52	X	C, S, DIC, TA	X	X	X	X	X	X	C		X						
M910/1743-2	F	ZODIAC													X					
M910/1744-1	F	CTD/RO	92	X	C, S, DIC, TA	X	X		X	X		C	X			X		X		
M910/1744-2	F	ZODIAC													X					
M910/1745-1	F	CTD/RO	109	X	C, S	X	X	X	X	X	X	C				X				
M910/1745-2	F	ZODIAC													X					
M910/1746-1	F	CTD/RO	139	X	C, S, DIC, TA	X	X	X	X	X	X	C	X			X		X		
M910/1746-3	F	ZODIAC													X					
M910/1747-1	F	CTD/RO	170	X	C, S	X	X	X	X	X		C				X				
M910/1748-1	F	CTD/RO	822	X	C, S, DIC, TA	X	X	X	X	X	X	C	X			X		X		
M910/1749-1	F	CTD/RO	1695	X		X	X		X	X		C	X			X		X		X
M910/1750-1	F	CTD/RO	2008	X	C, S	X	X	X	X	X	X	C	X	X		X				
M910/1750-3	F	ZODIAC													X					
M910/1751-1	F	CTD/RO	2006	X		X		X		X	X	C	X					X		
M910/1751-3	F	CTD/RO	174	X		X	X	X	X	X	X	C	X			X	X	X	X	
M910/1752-1	G	CTD/RO	5012	X		X				X			X	X						X
M910/1752-2	G	ZODIAC													X					
M910/1752-4	G	CTD/RO	174	X	U	X		X		X			X	X						

Stat#-Cast#	Tran-sect	Gear	CTD/RO m	Nut., O_2	(1)	(2)	(3)	(4)	(5)	(6)	(7)	(8)	(9)	(10)	(11)	(12)	(13)	(14)	(15)	(16)
M910/1752-5	G	ZODIAC													X					
M910/1752-7	G	ZODIAC								X										
M910/1752-8	G	CTD/RO	2006	X	U	X		X	X				X	X		X		X		X
M910/1752-9	G	ZODIAC													X					
M910/1752-12	G	CTD/RO	2005	X		X							X							X
M910/1753-1	G	CTD/RO	2007	X	U	X	X						X	X						
M910/1753-2	G	ZODIAC													X					
M910/1754-1	G	CTD/RO	2010	X	U	X	X	X	X				X			X		X		
M910/1754-2	G	ZODIAC													X					
M910/1755-1	G	ZODIAC													X					
M910/1755-2	G	CTD/RO	1088	X	U	X	X	X	X	X		O	X			X		X		
M910/1755-4	G	CTD/RO	181	X	U	X		X		X		O	X			X		X		
M910/1756-1	G	CTD/RO	194	X	U	X	X			X			X			X		X		
M910/1757-1	G	CTD/RO	88	X	U	X	X						X							
M910/1758-1	H	CTD/RO	67	X		X	X			X			X	X						
M910/1758-2	H	ZODIAC													X					
M910/1759-1	H	CTD/RO	98	X		X	X		X	X	X	O	X			X			X	
M910/1759-3	H	ZODIAC													X					
M910/1760-1	H	CTD/RO	98	X		X	X		X	X	X		X	X		X				
M910/1760-3	H	ZODIAC													X					
M910/1761-1	H	CTD/RO	90	X		X	X	X		X			X							X
M910/1761-2	H	ZODIAC													X					
M910/1761-3	H	ZODIAC													X					
M910/1762-1	H	ZODIAK													X					
M910/1762-2	H	CTD/RO	81	X		X	X	X	X	X	X	O	X			X	X	X	X	
M910/1763-1	I	CTD/RO	245	X		X	X		X	X			X			X				
M910/1764-1	I	CTD/RO	2252	X		X		X	X	X			X	X		X				X
M910/1764-3	I	CTD/RO	200	X		X	X	X		X			X	X						
M910/1764-4	I	ZODIAC													X					
M910/1764-6	I	ZODIAC								X										
M910/1764-7	I	ZODIAC													X					
M910/1764-8	I	CTD/RO	2007	X		X			X		X		X	X						X
M910/1764-9	I	ZODIAC													X					

Stat#-Cast#	Tran-sect	Gear	CTD/RO m	Nut., O_2	(1)	(2)	(3)	(4)	(5)	(6)	(7)	(8)	(9)	(10)	(11)	(12)	(13)	(14)	(15)	(16)
M910/1764-12	I	CTD/RO	2009	X		X							X	X						X
M910/1765-1	I	CTD/RO	2007	X		X	X	X	X				X	X		X				
M910/1765-2	I	ZODIAC													X					
M910/1766-1	I	CTD/RO	2007	X		X			X	X			X			X		X		
M910/1766-3	I	CTD/RO	175	X		X	X	X		X			X			X	X	X	X	
M910/1766-4	I	ZODIAC													X					
M910/1767-1	I	CTD/RO	--	--	--	--	--	--	--	--	--	--	--	--	--	--	--	--	--	--
M910/1767-2	I	CTD/RO	2007	X		X	X						X							
M910/1768-1	I	CTD/RO	2007	X		X				X	X		X			X		X		
M910/1768-3	I	CTD/RO	176	X		X	X			X	X		X					X		
M910/1769-1	Ia	CTD/RO	1003	X		X		X	X				X	X		X	X	X		
M910/1769-3	Ia	ZODIAC													X					
M910/1770-1	Ia	ZODIAC													X					
M910/1770-2	Ia	CTD/RO	1002	X		X	X		X	X	X	O	X							
M910/1770-4	Ia	CTD/RO	200	X		X				X	X	O	X			X				
M910/1771-1	Ia	CTD/RO	1003	X		X	X	X								X		X		
M910/1772-1	Ia	CTD/RO	1004	X		X	X	X		X			X							
M910/1772-3	Ia	ZODIAC													X					
M910/1773-2	J	CTD/RO	2013	X		X	X		X		X		X	X						X
M910/1773-3	J	CTD/RO	181	X		X			X		X		X	X						
M910/1773-5	J	CTD/RO	--	--	--	--	--	--	--	--	--	--	--	--	--	--	--	--	--	--
M910/1774-1	J	CTD/RO	2010	X		X			X				X							
M910/1774-3	J	CTD/RO	203	X		X	X						X			X	X	X	X	
M910/1775-1	J	CTD/RO	2011	X		X			X				X			X		X		
M910/1775-3	J	CTD/RO	176	X		X	X						X			X	X	X	X	X
M910/1776-1	J	CTD/RO	2009	X		X		X		X			X							
M910/1776-3	J	ZODIAC													X	X				
M910/1776-4	J	CTD/RO	199	X		X	X			X			X					X		
M910/1777-1	J	CTD/RO	2010	X		X			X	X	X		X	X		X		X		X
M910/1777-2	J	ZODIAC													X					
M910/1777-4	J	CTD/RO	200	X		X	X	X	X	X	X		X	X		X	X	X	X	
M910/1777-5	J	ZODIAC													X					
M910/1777-7	J	CTD/RO	2009	X		X							X			X				X

Stat#-Cast#	Tran-sect	Gear	CTD/RO m	Nut., O_2	(1)	(2)	(3)	(4)	(5)	(6)	(7)	(8)	(9)	(10)	(11)	(12)	(13)	(14)	(15)	(16)
M910/1777-10	J	ZODIAC								X										
M910/1777-11	J	CTD/RO	2011	X		X		X					X	X		X	X	X		X
M910/1778-1	J	CTD/RO	270	X		X	X	X	X	X	X		X			X	X	X	X	
M910/1778-3	J	ZODIAC												X						
M910/1778-4	J	CTD/RO	133	X		X				X			X							

24h stations are marked in bold.

8 Data and Sample Storage and Availability

The data were collected for the BMBF Verbundprojekt SOPRAN (Surface Ocean Processes in the Anthropocene). The SOPRAN data management is run by the Kiel Data Management Team (KDMT) at GEOMAR which organizes and supervises the storage and publication of SOPRAN data with a web-based multi-user system (portal). In a first phase data are only available to the project (i.e. M91) user groups. After a three year proprietary time the KDMT will publish M91 data by releasing them to national and international data archives such as PANGAEA (www.pangaea.de). The M91 data set will be released by 01 February 2016 at the latest. Digital object identifiers (DOIs) are automatically assigned to data sets archived in the PANGAEA Open Access library making them publically retrievable, citeable and reusable for the future.
All M91 metadata are immediately available from the GEOMAR portal: https://portal.geomar.de/metadata/leg/show/316029. In addition the GEOMAR portal provides a single downloadable KML formatted file (https://portal.geomar.de/metadata/leg/kmlexport/316029) which retrieves and combines up-to-date M91 related information and links to restricted data as well as to published data for visualization e.g. in GoogleEarth. Contact person for data access is Dr. Hermann W. Bange at GEOMAR Helmholtz-Zentrum fuer Ozeanforschung, Kiel.

9 Acknowledgements

We like to thank captain Thomas Wunderlich, his officers and crew of R/V Meteor for their support of our measurement programme and for creating a very friendly and professional work atmosphere on board. Moreover, we thank the Leitstelle Deutsche Forschungsschiffe for their support during the organisation of M91. The ship time of Meteor was provided by the German Science Foundation (DFG) within the core program Meteor/Merian. We thank two anonymous reviewers for their comments which helped to improve the cruise report. Funding for M91 was provided by the BMBF Verbundprojekt SOPRAN (Surface Ocean Processes in the Anthropocene; www.sopran.pangaea.de) via grant FKZ 03F0611A. SOPRAN is a German contribution to SOLAS (Surface Ocean – Lower Atmosphere Study; www.solas-int.org).

We thank the authorities of Peru for their generous permission to work in their territorial waters.

10 References

Altabet, M.A., 2001. Nitrogen isotopic evidence for micronutrient control of fractional NO_3^- utilization in the equatorial Pacific. Limnology and Oceanography 46, 368-380.

Andersen, A.T., Foyn, L., 1969. In: Lange, R., (Ed.), Chemical Oceanography, Universitetsforlaget, Oslo pp. 129-130.

Arp, D.J., Stein, L.Y., 2003. Metabolism of inorganic N compounds by ammonia-oxidizing bacteria. Critical Reviews in Biochemistry and Molecular Biology 38, 471-495.

Bahlmann, E., Weinberg, I., Seifert, R., Tubbesing, C., Michaelis, W., 2011. A high volume sampling system for isotope determination of volatile halocarbons and hydrocarbons. Atmos. Meas. Tech. 4, 2073-2086.

Baker, A. R., Weston, K., Kelly, S. D., Voss, M., Streu, P., Cape, J. N., 2007. Dry and wet deposition of nutrients from the tropical Atlantic atmosphere: links to primary productivity and nitrogen fixation. Deep-Sea Research Part I, 54, 1704-1720.

Bourbonnais, A., Lehmann, M.F., Butterfield, D.A., Juniper, S.K., 2012a. Subseafloor nitrogen transformations in diffuse hydrothermal vent fluids of the Juan de Fuca Ridge evidenced by the isotopic composition of nitrate and ammonium. Geochemistry Geophysics Geosystems 13, Q02T01, doi:10.1029/2011GC003863.

Bourbonnais, A., Lehmann, M.F., Waniek, J.J., Schulz-Bull, D.E., 2009. Nitrate isotope anomalies reflect N_2 fixation in the Azores Front region (subtropical NE Atlantic). Journal of Geophysical Research 114, C03003, doi: 10.1029/2007JC004617.

Brandes, J.A., Devol, A.H., Yoshinari, T., Jayakumar, D.A., Naqvi, S.W.A., 1998. Isotopic composition of nitrate in the central Arabian Sea and eastern tropical North Pacific: A tracer for mixing and nitrogen cycles. Limnology and Oceanography 43, 1680-1689.

Broadgate, W.J., Liss, P.S., Penkett, S.A., 1997. Geophys. Res. Lett. 24, 2675–2678.

Butler, J.H., King, D.B., Lobert, J.M., Montzka, S.A. Yvon-Lewis, S.A., Hall, N B.D., Warwick, J., Mondeel, D.J., Aydin, M., Elkins, J.W., 2007. Oceanic distributions and emissions of short-lived halocarbons. Global Biogeochem. Cycles 21, GB1023, doi: 10.1029/2006GB002732.

Butler, J.H., Gordon, L.I., 1986. Rates of nitrous oxide production in the oxidation of hydroxylamine by iron (III). Inorganic Chemistry 25, 4573-4577.

Cabello, P., Roldan, M.D., Moreno-Vivian, C., 2008. Nitrate reduction and the nitrogen cycle in archaea. Microbiology 150, 3527-3546.

Capone, D., 2008. The marine nitrogen cycle. Microbe 3, 2008.

Carpenter, L.J., Liss, P.S., 2000. On temperate sources of bromoform and other reactive organic bromine gases. J. Geophys. Res. 105, 20,539-20,547.

Casciotti, K.L., McIlvin, M.R., 2007. Isotopic analyses of nitrate and nitrite from reference mixtures and application to eastern tropical North Pacific waters. Marine Chemistry 107, 184-201.

Charlson, R.J., Lovelock, J.E., Andreae, M.O., Warren, S.G., 1987. Oceanic phytoplankton, atmospheric sulphur, cloud albedo and climate. Nature 326, 655-661.

Cline, J.D., Kaplan, I.R., 1975. Isotopic fractionation of dissolved nitrate during denitrification in the eastern tropical north pacific ocean. Marine Chemistry 3, 271-299.

Class, T., Ballschmiter, K., 1988. Chemistry of organic traces in air. J. Atmos. Chem., 6, 35.

Coble, P., 1996. Characterization of marine and terrestrial DOM in seawater using excitation-emission matrix spectroscopy. Mar. Chem. 51, 325-356.

Codispoti, L.A., 2007. An oceanic fixed nitrogen sink exceeding 400 Tg N a^{-1} vs the concept of homeostasis in the fixed-nitrogen inventory. Biogeosciences 4, 233-253.

Collén, J., Ekdahl, A., Abrahamsson, K., Pedersén, M., 1994. The involvement of hydrogen peroxide in the production of volatile halogenated compounds by *Meristiella Gelidium*. Phytochemistry 36, 1197-1202.

Cunliffe, M. Murrell, J.C., 2009. The sea-surface microlayer is a gelatinous biofilm. ISME Journal 3, 1001-1003.

Deutsch, C., Sarmiento, J.L., Sigman, D.M., Gruber, N., Dunne, J.P., 2007. Spatial coupling of nitrogen inputs and losses in the ocean. Nature 445, 163-167.

Dickson A.G., 1993. The measurement of sea water pH. Marine Chemistry 44, 131-142.

DOE, 1994. Handbook of methods for the analysis of the various parameters of the carbon dioxide system in sea water, version 2, Dickson A.G., Goyet, C., (Eds.) ORNL/CDIAC-74.

Engel, A., Händel, N., 2011. A novel protocol for determining the concentration and composition of sugars in particulate and in high molecular weight dissolved organic matter (HMW-DOM) in seawater. Marine Chemistry 127, 180-191.

Engel, A., 2009. Determination of marine gel particles. In: Practical guidelines for the analysis of seawater. CRC Press.

Fischer, E.V., Jacob, D.J., Millet, D., Yantosca, R.M., Mao, J., 2012. Geophys. Res. Lett. 2012, 39.

Fuenzalida, R., Schneider, W., Garcés-Vargas, J., Bravo, L., Lange, C., 2009. Vertical and horizontal extension of the oxygen minimum zone in the eastern South Pacific Ocean. Deep-Sea Research Part II 56, 992-1003.

Fuhlbrügge, S., Krüger, K., Quack, B., Atlas, E.L., Hepach, H., Ziska, F., 2012. Impact of the marine atmospheric boundary layer on VSLS abundances in the eastern tropical and subtropical North Atlantic Ocean. Atmospheric Chemistry and Physics Discussions 12, 31205-31245.

Gebhardt, S., Walter, S., Nausch, G., Bange, H.W., 2004. Hydroxylamine (NH_2OH) in the Baltic Sea. Biogeosciences Discussions 1, 709-724.

Hepach, H., Quack, B., Ziska, F., Fuhlbrügge, S., Atlas, E.L., Peeken, I., Krüger, K., Wallace, D.W.R., 2013. Drivers of diel and regional variations of halocarbon emissions from the tropical Northeast Atlantic, in preparation.

Falkowski, P.G., 1997. Evolution of the nitrogen cycle and its influence on the biological sequestration of CO_2 in the ocean. Nature 387, 272-275.

Friederich, G., Ledesma, J., Ulloa, O., Chavez, F.P., 2008. Air-sea carbon dioxide fluxes in the coastal southeastern tropical Pacific. Progress in Oceanography 79, 156–166.

Frieß, U., Monks, P.S., Remedios, J.J., Rozanov, A., Sinreich, R., Wagner, T., Platt, U., 2006. MAX-DOAS O_4 measurements: A new technique to derive information on atmospheric aerosols. J. Geophys. Res.

Gantt, B., Meskhidze N., Kamykowski, D., 2009. Atmos. Chem. Phys. 9, 4915–4927.

Gist, N., Lewis, A.C., 2006. Mar. Chem. 100, 1-10.

Granger, J., Sigman, D.M., Lehmann, M.F., Tortell, P.D., 2008. Nitrogen and oxygen isotope fractionation during dissimilatory nitrate reduction by denitrifying bacteria. Limnology and Oceanography 53, 2533-2545.

Großmann, K., Frieß, U., Peters, E., Wittrock, F., Tschritter, J., Quack, B., Krüger, K., Sommariva, R., von Glasow, R., Pfeilsticker, K., Platt, U., 2012. Iodine monoxide in the western Pacific marine boundary layer. Atmos. Chem. Phys. Discuss.

Gschwend, P.M., MacFarlane, J.K., Newman, K.A., 1985. Volatile halogenated organic compounds released to seawater from temperate marine macroalgae. Science 227, 1033-1035.

Harper, D.B., Hamilton, J.T.G., Ducrocq, V., Kennedy, J.T., Downey, A., Kalin, R.M., 2003. The distinctive isotopic signature of plant-derived chloromethane: possible application in constraining the atmospheric chloromethane budget. Chemosphere 52, 433-436.

Hoffmann, L.J., Peeken, I., Lochte, K., Assmy, P., Veldhuis, M., 2006. Different reactions of southern ocean phytoplankton size classes to iron fertilization. Limnol. Oceanogr. 51, 1217-1229.

Hossaini, R., Chipperfield, M.P., Feng, W., Breider, T.J., Atlas, E., Montzka, S.A., Miller, B.R., Moore, F., Elkins, J., 2012. The contribution of natural and anthropogenic very short-lived species to stratospheric bromine. Atmos. Chem. Phys. 12, 371-380.

Hughes, C., Franklin, D. J., Malin, G., 2011. Iodomethane production by two important marine cyanobacteria: *Prochlorococcus marinus* (CCMP 2389) and *Synechococcus sp* (CCMP 2370). Marine Chemistry 125, 19-25.

Karlsson, A., Auer, N., Schulz-Bull, D., Abrahamsson, K., 2008. Cyanobacterial blooms in the Baltic - A source of halocarbons. Marine Chemistry 110, 129-139.

Keppler, F., Harper, D.B., Röckmann, T., Moore, R.M. Hamilton, J.T.G, 2005. New insight into the atmospheric CH_3Cl budget gained using stable carbon isotope ratios. Atmospheric Chemistry and Physics 5, 2403-2411.

Knapp, A.N., Sigman, D.M., Lipschultz, F., 2005. N isotopic composition of dissolved organic nitrogen and nitrate at the Bermuda Atlantic time-series Study site. Global Biogeochemical Cycles 19, GB1018, doi:10.1029/2004GB002320.

Kock, A., Bange H.W., 2013. Nitrite removal improves hydroxylamine analysis in aqueous solution by conversion with iron(III). Environmental Chemistry, accepted.

Kock, A., Schafstall, J., Dengler, M., Brandt, P., Bange H.W., 2012. Sea-to-air and diapycnal nitrous oxide fluxes in the eastern tropical North Atlantic Ocean. Biogeosciences 9, 957-964.

La Barre, S., Potin, P., Leblanc, C., Delage, L., 2010. The halogenated metabolism of brown algae (Phaeophyta), its biological importance and its environmental significance. Marine Drugs 8, 988-1010.

Laturnus, F., 2001. Marine macroalgae in polar regions as natural sources for volatile organohalogens. Environ. Sci. Pollut. Res. 8, 103-108.

Lewis, A.C., Hopkins, J.R., Carpenter, L.C., Stanton, J., Read K.A., Pilling, M.J., 2005. Atmos. Chem. Phys. 5, 1963–1974.

Liang, Q., Stolarski, R.S., Kawa, S.R., Nielsen, J.E., Rodriguez, J.M., Douglass, A.R., Blake, D.R., Atlas, E.L. Ott, L.E., 2010. Finding the missing stratospheric Bry: A global modeling study of CHBr3 and CH2Br2. Atmos. Chem. Phys. 10, 2269-2286.

Liss, P.S., Duce, R.A., 1997. The sea surface and global change. Cambridge University Press.

Löscher, C.R., Kock, A., Könneke, M., LaRoche, J., Bange, H.W., Schmitz, R.A., 2012. Production of oceanic nitrous oxide by ammonia-oxidizing archaea. Biogeosciences 9, 2419-2429.

Luo G., Yu, F., 2010. Atmos. Chem. Phys. 10, 2007–2015.

McIlvin, M.R., Altabet, M.A., 2005. Chemical conversion of nitrate and nitrite to nitrous oxide for nitrogen and oxygen isotopic analysis in freshwater and seawater. Analytical Chemistry 77, 5589–5595.

McIlvin, M.M., Casciotti, K. L., 2010. Automated stable isotopic analysis of dissolved nitrous oxide at natural abundance levels. Limnology and Oceanography- Methods 8, 54–66.

McLinden, C.A., 2005. Sensitivity of ozone to bromine in the lower stratosphere. Geophys. Res. Lett. 32, L05811, doi: 10.1029/2004gl021504.

Meyer, S., 2009. Entwicklung einer Methode zur Messung von Hydrazin in Seewasser, Diploma Thesis, 64 pp., Universität Kiel, Kiel.

Mueller, M., George, C., D'Anna, B., 2011. Int. J. Mass Spec. 306, 1-8.

Mueller, M., Graus, M., Ruuskanen, T.M., Schnitzhofer, R., Bamberger, I., Kaser, L., Titzmann, T., Hoertnagl, L., Wohlfahrt, G., Karl, T., Hansel, A., YEAR. Atmos. Meas. Tech. 3, 387-395.

O'Brien L.M., Palmer, C.J., Reason, C.J., 2009. Relationships of surface CHBr3 concentrations with mixed layer depth and salinity in the tropical oceans. Global Biogeochem. Cycles 23, GB2014, doi: 10.1029/ 2008GB003338.

O'Dowd, C.D., Jimenez, J.L., Bahreini, R., Flagan, R.C., Seinfeld, J.H., Hameri, K., Pirjola, L., Kulmala, M., Jennings, S.G., Hoffmann, T., 2002. Marine aerosol formation from biogenic iodine emissions. Nature, 417, 632-636.

Palmer, C.J., Reason, C.J., 2009. Relationships of surface depth and salinity in the tropical oceans. Global Biogeochem. Cycles 23, GB2014, doi: 10.1029/ 2008GB003338.

Paulmier, A., Ruiz-Pino, D., Garcon, V., 2008. The oxygen minimum zone (OMZ) off Chile as intense source of CO_2 and N_2O. Continental Shelf Research 28, 2746-2756.

Piontek, J., Lunau, M., Händel, N., Borchard, C., Wurst, Engel, A., 2010. Acidification increases microbial polysaccharide degradation in the ocean. Biogeosciences 7, 1615-1624.

Platt, U., Stutz, J., 2008. Differential optical absorptions spectroscopy. Springer Verlag.

Platt, U., Meinen, J., Pöhler, D., Leisner, T., 2009. Broadband cavity enhanced differential optical absorption spectroscopy (CE-DOAS) - applicability and corrections. Atmos.Meas. Tech. 2,713–723.

Quack, B., Atlas, E., Petrick, G., Schauffler, S, Wallace D.W.R., 2004. Oceanic CHBr3 sources for the tropical atmosphere. Geophys. Res. Lett., doi: 10.1029/2004GL020597.

Quack, B., Atlas, E., Petrick, G., Wallace, D.W.R., 2007a. Bromoform and dibromomethane above the Mauritanian upwelling: Atmospheric distributions and oceanic emissions. J. Geophys. Res. 112, D09312, doi: 10.1029/2006jd007614.

Quack, B., Peeken, I., Petrick, G., Nachtigall, K., 2007b. Oceanic distribution and sources of bromoform and dibromomethane in the Mauritanian upwelling. J. Geophys. Res. 112, C10006, doi: 10.1029/2006jc003803.

Read, K.A., Mahajan, A.S., Carpenter, L. J., Evans, M.J., Faria, B.V.E., Heard, D.E., Hopkins, J.R., Lee, J.D., Moller, S.J., Lewis, A.C., Mendes, L., McQuaid, J.B., Oetjen, H., Saiz-Lopez, A, Pilling, M.J., Plane, J.M.C., 2008. Extensive halogen-mediated ozone destruction over the tropical Atlantic Ocean. Nature 453, 1232-1235.

Rhein, M., Dengler, M., Sültenfuß, J., Hummels, R., Hüttl-Kabus, S., Bourles, B., 2010. Upwelling and associated heat flux in the equatorial Atlantic inferred from helium isotope disequilibrium. J Geophys. Res., 115, C08021, doi: 10.1029/2009JC005772.

Richter, U., Wallace, D.W.R., 2004. Production of methyl iodide in the tropical Atlantic Ocean. Geophys. Res. Lett. 31, L23s03, doi: 10.1029/2004gl020779.

Salawitch, R.J., Weisenstein, D.K., Kovalenko, L.J., Sioris, C.E., Wennberg, P.O., Chance, K., Ko, M.K.W., McCauley, S.E., Goldstein, A.H., DePaolo, D.J., 1999. An isotopic approach for understanding the CH3Br budget of the atmosphere. Proceedings of the National Academy of Sciences of the United States of America 96, 10006-10009.

Santoro, A.E., Buchwald, C., McIlvin, M.R., Casciotti, K.L., 2011. Isotopic Signature of N_2O produced by marine ammonia-oxidizing archaea. Science 333, 1282-1285.

Scarratt, M.G., Moore, R.M., 1996. Production of methyl chloride and methyl bromide in laboratory cultures of marine phytoplankton. Marine Chemistry 54, 263-272.

Schauffler, S.M., Atlas, E.L., Blake, D.R., Flocke, F., Lueb, R.A., Lee-Taylor, J.M., Stroud, V., Travnicek, W., 1999. Distributions of brominated organic compounds in the troposphere and lower stratosphere. J. Geophys. Res. 104, 21,513-21,535.

Schönhardt, A., Begoin, M., Richter, A., Wittrock, F., Kaleschke, L., Gómez Martín, J.C., Burrows, J.P., 2012. Simultaneous satellite observations of IO and BrO over Antarctica. ACP, 2012.

Sieburth, J.M., 1983. Microbiological and organic-chemical processes in the surface and mixed layers. IN: Air-sea exchange of gases and particles. D. Reidel Publishing Company.

Sigman, D.M., Casciotti, K.L., Andreani, M., Barford, C., Galanter, M., Bohlke, J.K., 2001. A bacterial method for the nitrogen isotopic analysis of nitrate in seawater and freshwater. Analytical Chemistry 73, 4145–4153.

Sigman, D.M., Granger, J., DiFiore, P.J., Lehmann, M.M., Ho, R., Cane, G., van Geen, A., 2005. Coupled nitrogen and oxygen isotope measurements of nitrate along the eastern North Pacific margin. Global Biogeochemical Cycles 19.

Simó, R., 2001. Production of atmospheric sulfur by oceanic plankton: biogeochemical, ecological and evolutionary links. TRENDS in Ecology & Evolution 16, 287-293.

Sinreich, R., Coburn, S., Dix, B., Volkamer, R., 2010. Ship-based detection of glyoxal over the remote tropical Pacific Ocean. Atmos. Chem. Phys.

Stedmon, C.A, Bro, R., 2008. Characterizing dissolved organic matter fluorescence with parallel factor analysis: A tutorial. Limnology and Oceanography - Methods 6, 572-579.

Stefels J.; M. Steinke, S. Turner, G. Malin, S. Belviso. 2007. Environmental constraints on the productionn and removal of the climatically active gas dimethylsulphide (DMS) and implications for ecosystem modeling. Biogeochemistry 83, 245-275.

Steinhoff, T., Bange, H.W., Kock, A., Wallace, D.W.R., Körtzinger, A., 2012. Biological productivity in the Mauritanian upwelling estimated with a triple gas approach. Biogeosciences Discuss. 9, 4853-4875.

Stramma, L., Johnson, G.C., Sprintall, J., Mohrholz, V., 2008. Expanding oxygen-minimum zones in the tropical oceans. Science 320, 655-658.

Titzmann, T., Graus, M., Mueller, M., Hansel, A., Ostermann, A., 2012. Int. J. Mass Spectrom. 295, 72-77.

Vogt, R., Sander, R., Von Glasow, R., Crutzen, P.J., 1999. Iodine chemistry and its role in halogen activation and ozone loss in the marine boundary layer: A model study. J. Atmos. Chem. 32, 375-395.

Voss, M., Dippner, J.W., Montoya, J.P., 2001. Nitrogen isotope patterns in the oxygen-deficient waters of the Eastern Tropical North Pacific Ocean. Deep Sea Research Part I 48, 1905-1921.

Utermöhl, H., 1958. Zur Vervollkomnung der quantitativen Phytoplankton-Methodik. Mitt. Inter. Ver. Limnol. 9, 1-38.

Vrekoussis, M., Wittrock, F., Richter, A., Burrows, J.P., 2009. Temporal and spatial variability of glyoxal as observed from space. Atmos. Chem. Phys.

Winkler. L.W., 1888. Ber. Dtsch. Chem. Ges. 20, 291.

WMO (World Meteorological Organization), Scientific Assessment of Ozone Depletion (2010) Global Ozone Research and Monitoring Project–Report No. 52, 516 pp., Geneva, Switzerland

Yoshida, N., Toyoda, S., 2000. Constraining the atmospheric N_2O budget from intramolecular site preference in N_2O isotopomers. Nature 405, 330–334.

Yoshinari, T., Altabet, M.A., Naqvi, S.W.A., Codispoti, L., Jayakumar, A., Kuhland, M., Devol, A., 1997. Nitrogen and oxygen isotopic composition of N_2O from suboxic waters of the eastern tropical North Pacific and the Arabian Sea – Measurements by continuous-flow isotope ratio monitoring. Marine Chemistry 56, 253–264.

Zhang, L., Altabet, M.A., Wu, T., Hadas, O. 2007. Sensitive measurement of NH_4 $^{15}N/^{14}N$ ($^{15}NH_4$) at natural abundance levels in fresh and saltwaters. Analytical Chemistry 79, 5297–5303.